ORIGINAL SCIENTIFIC PAPER

CROATICA CHEMICA ACTA

Croat. Chem. Acta **2026**, *99*(1)
Published online: May 19, 2026
DOI: 10.5562/cca4215

HKD 1926

Comprehensive Tutorial: Characterization of Small Molecule–DNA Noncovalent Binding Interactions

Gordan Horvat,[1,*] Ivo Piantanida[2,#]

[1] Department of Chemistry, Faculty of Science, University of Zagreb, Horvatovac 102a, HR-10000 Zagreb, Croatia
[2] Division of Organic Chemistry and Biochemistry, Ruđer Bošković Institute, Bijenička cesta 54, HR-10000 Zagreb, Croatia
* Corresponding author's e-mail address: ghorvat@chem.pmf.hr
# Corresponding author's e-mail address: pianta@irb.hr

RECEIVED: October 06, 2025 ✶ REVISED: February 27, 2026 ✶ ACCEPTED: February 27, 2026

PROCEEDING OF THE SOLUTIONS IN CHEMISTRY 2024, 11–15 NOVEMBER 2024, SVETI MARTIN NA MURI, CROATIA

Abstract: Non-covalent interactions between small molecules and nucleic acids are essential to many biological processes and the function of numerous therapeutic and diagnostic agents. These interactions are complex due to the structural diversity of DNA / RNA forms and the variety of possible binding modes. Factors such as nucleic acid topology, sequence, ionic conditions, and ligand aggregation further complicate analysis. Because no single technique can capture the full picture, a combination of spectroscopic and biochemical methods is required for accurate characterization. By combining working principles of four most common and available experimental methods with interpretative guidance and methodological details, this tutorial aspires to be a comprehensive reference for both novice and experienced researchers working in the field of small molecule–nucleic acid interactions. All discussed concepts apply equally to other types of DNA or RNA, and are generally relevant to most non-covalent ligand–biomolecule (including protein) interactions.

Keywords: non-covalent binding to DNA, UV-Vis, fluorescence, thermal denaturation, circular dichroism, indicator displacement assay.

INTRODUCTION

NON-COVALENT interactions between small molecules (ligands) and nucleic acids (DNA and RNA) are central to numerous biological processes and have long been a foundation for the development of therapeutic agents, biochemical tools, and molecular probes used to modulate or investigate nucleic acid structure and function.[1,2] Many clinically important drugs—such as actinomycin D, daunorubicin, and cisplatin analogs—as well as naturally occurring antibiotics and antiviral agents function through binding to DNA or RNA via covalent or non-covalent mechanisms.[3,4,5]

However, the nature of the complexes formed between a relatively small ligand and the much larger, structurally diverse targets such as DNA or RNA, often containing unknown number of binding sites, may be considerably complicated. This complexity arises not only from the diversity of nucleic acid conformations (duplexes, triplexes, G–quadruplexes, etc.) but also from the multiple potential binding modes a ligand can adopt simultaneously or consecutively (intercalation, groove binding, external stacking, etc. Scheme 1). The formation of these complexes is further complicated by factors such as DNA / RNA topology, ionic strength, sequence context, and ligand aggregation ability.[1,4,5]

General Considerations Prior to Experimental Assessment and Analysis of the Results

Binding, non-binding and repulsive / steric interactions in the ligand / DNA complex are exceptionally complicated due to mutual impact on each other and strong influence of a solvent (water) and ionic species (buffer cations and anions). Moreover, DNA itself is very dynamic structure, DNA base pairs open and close spontaneously due to thermal fluctuations in a process known as DNA breathing.[12,13] While most DNA-breathing events occur on micro- to millisecond timescales, defects, triplex

formations, and external conditions can stretch breathing and structural transitions into second-long timescales. Moreover, DNA tends to some extent to adapt binding site shape to the ligand molecule requirements,[14,15] for instance allowing threading intercalators to bind.[9,10]

Thus, the formation of a non–covalent ligand–DNA complex is a highly intricate process that, in most cases, is not fully understood. For the purposes of this general tutorial, we will focus on several of the most extensively studied binding interactions at biorelevant conditions (room temperature or 37 °C, biorelevant ionic strength of pH 5–8 buffered solutions) and discuss their role in determining the overall binding mode.[16,17]

Scheme 1. A schematic presentation common non-covalent binding modes of small molecule to ds-DNA (LEFT to RIGHT):[1] intercalation,[1,6] electrostatic DNA–backbone association[1,2,4] or minor groove binding,[1,7] as well as some other less frequent binding modes, like partial intercalation,[8] threading intercalation[9,10] or major groove binding.[11]

LIGAND CHARGE

Over 99 % of all DNA-binding small molecules are positively charged,[1,4] stressing the importance of electrostatic interaction with polyanionic DNA backbone. However, the contribution of multicationic substituents attached to the ligand on the binding affinity (K_s) toward DNA is far from proportional to the number of positive charges;[18] due to many steric and repulsive effects. Very few ligands rely solely on the interaction with the polyanionic DNA backbone; however, many ligands have a positively charged appendage. As a rule of thumb, each positive charge on the ligand contributes by roughly 5 ± 1 kJ mol^{-1} to standard Gibbs free energy of binding[19] and thus increases the binding constant by roughly an order of magnitude. The contribution of positive charges induced by protonation of amines is strongly dependent on a p*K* value of the amine and its changes within the DNA binding site.

LIGAND AROMATIC SURFACE

Concept of minimal intercalator was intensively studied and so far, showing that minimal intercalators typically consist of small, planar aromatic cores (at least bicyclic, mostly tricyclic), with adequately positioned substituents to allow efficient DNA intercalation: most often presented by parallel orientation of ligand longer axis with longer axes of adjacent basepairs. The binding is then dominantly controlled by the interaction of aromatic systems,[1,4,20] and roughly yields binding constant of $K_s \sim 10^4$ M^{-1} order of magnitude for the smallest (bicyclic) aromatic system, tricyclic systems yielding $K_s \sim 10^5$–10^6 M^{-1} range (curved condensed aromatics preferred) and four-or five-condensed aromatics reaching up to $K_s \sim 107$ M^{-1}, which is actually limit defined by the aromatic surface of DNA–basepairs. However, bis- and multi-intercalators can significantly multiply affinity.[21,22]

HYDROPHOBICITY

Hydrophobicity is a one of key determinants of how small molecules approach and interact with DNA—modulating their binding affinity of the complex, and can even cause DNA–helix condensation or precipitation. Both the molecule's and DNA's hydrophobic features need to be considered.[23,24,25]

HYDROGEN BONDING INTERACTIONS

Some small molecules, natural products (e.g. netropsin, distamycin) or synthetic analogues[26] bind within the minor groove of DNA and use highly DNA : sequence-selective hydrogen bonding network with functional groups on the DNA bases, which allows them to target particular DNA–sequences. DNA major groove H–bonding recognition is common for proteins. Hydrogen bonds are very directional (180 ± 30°), mostly effective at short distance (2–3 Å) and can contribute to the DNA–binding only in the absence of bulk water, so even small conformational shifts or the presence of water molecules can weaken or eliminate the interaction. Therefore, it is generally not possible to estimate their contribution to the binding affinity of a ligand toward DNA.

VAN DER WAALS INTERACTIONS

Van der Waals (vdW) interactions sometimes have a critical but often underappreciated role in the binding of small molecules to DNA. The vdW interaction strength is highly dependent on the distance between interacting molecular orbitals, specifically following an inverse sixth-power relationship ($\propto 1 / r^6$), where *r* is the distance between the centers of the two interacting atoms or molecules. Although individually weak, VdW forces can be significant in large numbers—particularly in molecular recognition of ligand-DNA interactions, provided the involved atoms are in very close proximity (typically ~ 3–4 Å).[25,27,28] Thus, the key-and-lock principle could adequately describe the positive impact of exact shape match between the ligand and DNA-binding site, due to the short-range nature of VdW forces and their sensitivity to molecular geometry and conformational fit. Particularly Dipole-induced dipole interactions play a subtle but sometimes essential role in

molecule–DNA binding. They influence ligand orientation, binding energy, solvent mediation, and even higher-order DNA structure. These forces often act in tandem with or in competition with hydrogen bonding and π-stacking, and are especially relevant in systems involving polarizable environments or charged ligands.[29]

Because no single analytical method can fully characterize the complexity of ligand–nucleic acid interactions, accurate interpretation relies on integrating multiple complementary techniques. While a wide range of methods has been applied to study ligand / DNA binding, only a limited number are widely accessible. By combining these, researchers can obtain reliable information on complex stability, stoichiometry, binding modes, and the orientation of ligands within DNA binding sites. Most commonly, spectroscopic approaches—such as UV–Vis absorption, fluorescence, circular dichroism (CD), and linear dichroism (LD)—are employed to probe these interactions. In addition, thermal denaturation assays and fluorescence displacement methods (e.g., indicator displacement assays, IDA) provide essential insights into binding stability, modes, and specificity.

However, this set of methods comes with its own limitations regarding sensitivity, resolution, and susceptibility to artifacts. Misinterpretations are common when experimental conditions are not carefully optimized or when critical controls are omitted. For instance, changes in fluorescence intensity may be due to inner filter effects or ligand aggregation rather than genuine DNA binding. Similarly, CD spectral changes can be misleading if ligand-induced DNA conformational changes are incorrectly attributed to specific binding modes.[30]

Recognizing these challenges, several method-specific tutorials have emerged. A notable example is the step-by-step guide on using circular dichroism to monitor DNA conformational changes upon ligand binding.[31] A similar tutorial was very recently given for LD experiments,[32] and also a general outline on how to interpret CD and LD results with respect to the most common ligand–DNA binding modes was summarised on a more comparative basis.[33] A detailed and concise review concerning the evaluation of the DNA binding constants by titration fluorescence spectroscopy was recently published.[34] The authors examine key experimental factors and propose a reference protocol that can be used to standardize procedures for determining nucleic acid binding equilibrium constants. They then fit the experimental data using various methods and analyze the results, focusing on the statistical dispersion of the data to highlight the strengths and weaknesses of each fitting approach. Also, the comprehensive review was presented for DNA / RNA thermal denaturation experiments.[35] However, general assessment of the data obtained by several different methods was summarised more than 20 years ago,[36] not including recent advancements in methods or instruments.

The objective of the present review is to consolidate these fragmented insights into an updated, unified, and practical tutorial focused on the thermodynamic equilibrium small molecule / DNA complexes (not a kinetics of the binding process). We aim to provide detailed guidance on the experimental design, data collection, and interpretation strategies for a range of widely accessible techniques, particularly those that are comparatively fast, cost-effective common in chemical and biochemical laboratories. Special emphasis is placed on methods such as UV–Vis absorption, fluorescence spectroscopy, CD spectropolarimetry, applied either for titrations, thermal denaturation, or indicator displacement assay (IDA).

Importantly, we also address less commonly discussed but increasingly relevant phenomena such as ligand aggregation and its impact on nucleic acid binding. There is an increasing number of cases when ligand aggregation in the DNA binding site plays a biorelevant role. For example, while netropsin typically binds as a monomer within the minor groove of AT–rich DNA, its structural analog distamycin preferentially binds as a dimer—demonstrating that small changes in ligand structure or concentration can dramatically alter binding behavior.[37,38] This concept was used in a particularly elegant application of synthetic polyamides self-assembly within the DNA minor groove.[39]

By combining methodological detail with interpretative guidance, this tutorial aspires to be a comprehensive reference for both novice and experienced researchers working in the field of small molecule–nucleic acid interactions. For simplicity, we will refer to double-stranded (ds) DNA as the "host" or "target" throughout this text. However, all concepts discussed apply equally to other types of poly-stranded DNA or RNA, even single stranded (ss) DNA / RNA, and are generally relevant to most non-covalent ligand–biomolecule (including protein) interactions.

GENERAL CONSIDERATIONS IN LIGAND–DNA/RNA INTERACTION STUDIES

Accurate and reproducible characterization of small molecule–DNA / RNA interactions critically depends on the physico-chemical and spectroscopic properties of both binding partners. Namely, even subtle impurities, aggregation, or DNA–misfolding can lead to inaccurate results, misinterpretation of binding behavior, or failure to detect meaningful interactions. Therefore, it is essential

that prior to any biophysical or spectroscopic analysis, purity, structural integrity, and physicochemical properties of both the ligand (small molecule) and the host (DNA or RNA) should be characterized by standard set of methods, as proposed in further text.

Purity and Characterization of Ligands and DNA (Host)

LIGANDS (SMALL MOLECULES)

Spectrophotometric techniques (UV–Vis absorbance, CD, fluorescence) commonly require a concentration-proportional response of chromophore in the working concentration range. Failure to establish linearity can result in incorrect determination of binding stoichiometry and binding constants. Therefore, ligands should meet further requirements:

Purity: While more complex ligands (such as isolated natural products or intricate peptidoids) are often difficult to obtain at > 99 % purity, a minimum of 95 % purity is generally required for reliable studies of biorelevant interactions. This level is typically achieved through chromatography or recrystallization and verified using HPLC coupled with mass spectrometry or UV–Vis detectors, and / or NMR spectra analysis and / or in particular cases by UV–Vis spectroscopy. However, in fluorescence experiments, even 99.9 % purity may be inadequate, since trace impurities with higher fluorescence quantum yields than the dye under study can still distort results.[41] Thus, additional check by collecting excitation spectrum (expected to excellently overlap with UV–Vis spectrum of a dye) should be performed.

Solubility and solvent impact: Ligand solubility must be checked under biorelevant experimental conditions, similar to those further used in biological assays: if possible, dissolve DNA and ligand in the same buffer to avoid mixing artifacts. However, non-adequate solubility of ligands in aqueous solution could eventually be circumvented by careful use of stock solutions prepared in an appropriate solvent (e.g., DMSO, ethanol), ensuring this solvent concentration in further experiments does not interfere with the experiment. For instance, the most common and efficient solvent is DMSO, however its impact on biochemical studies was characterized many decades ago, and is hard to find in recent literature. DMSO does not interfere significantly with DNA or RNA properties up to 0.1 % *v*/*v*,[40] while at higher volume fractions DMSO decreases the thermal stability of ds-DNA and also other poly stranded forms. Moreover, the DMSO impact on fluorescence or CD spectra should be corrected for, because DMSO significantly absorbs light < 240 nm, hampering accurate collection of data in the short-wavelength region due to absorbance and consequent inner filter effect (see below). A ligand stock solution in DMSO (commonly 0.001–0.01 M) should be clear and homogeneous with no visible precipitation or opalescence and checked for stability under storage conditions (commonly in the dark, +8 °C).

UV-Vis spectral characterization: Molar absorption coefficients should be determined with high accuracy by plotting absorbance against concentration (typically 0.5–50 μM) and applying linear regression, ensuring an R^2 value greater than 0.99. This parameter is critical, as all concentration-dependent measurements (e.g., verifying ligand concentrations in diluted solutions) rely on it. The pH-sensitive ligands should be thoroughly characterized by recording UV–Vis absorption spectra across a range of pH values, allowing shifts in absorption maxima and intensity to be monitored as a function of protonation state. From these spectra, pK_a values should be determined, either by fitting titration curves obtained from absorbance changes or by using appropriate computational/analytical methods. Accurate knowledge of the pK_a values and spectral behavior is essential for interpreting ligand–target interactions under physiological conditions, where small pH variations can significantly influence binding affinity and optical properties.

Fluorescence spectroscopy is highly sensitive and widely used for DNA–ligand interaction studies, but it is also the most prone to artifacts. As emphasized in the seminal work by Joseph R. Lakowicz in Principles of Fluorescence Spectroscopy, care must be taken to control for the following issues.[41]

Temperature stability: Emission of many fluorophores is temperature-sensitive—always maintain constant sample temperature.

Inner filter effects: When the total absorbance of a sample at the excitation wavelength exceeds 0.1, fluorophore molecules located farther from the light source receive reduced excitation intensity. Additionally, if the Stokes shift is small, part of the emitted light may be reabsorbed at excitation wavelength. Such inner filter effects can arise either from excessive ligand concentration or from increasing absorbance of a titrant (e.g., DNA) at the excitation wavelength. These artifacts can be minimized by employing a front-face excitation geometry in the fluorimeter,[42] or eventually corrected for by available algorithms.[43]

Scattering effects of solutions overlapping with the ligand spectrum: In fluorescence titrations, it is generally essential to check for scattering effects in order to ensure that observed signals originate from the ligand rather than from artifacts. A standard control is to record baseline spectra of DNA–only and buffer-only samples, excited at the same wavelength as the ligand, to identify contributions from Rayleigh or Raman scattering. To further reduce

overlap between excitation light and emission detection, it is advisable to begin monitoring fluorescence at least 10 nm above the excitation wavelength (or 20 nm if wider slits are employed). Several additional strategies can help minimize scattering artifacts, including the use of optical filters, narrow slit widths, or front-face illumination geometry; careful matching of solvent and cuvette quality; and, where possible, mathematical correction of background baselines. These precautions collectively ensure more reliable interpretation of fluorescence data in ligand–DNA binding studies.[41,44–46] Particular attention should be paid to: a) Rayleigh scattering in the wavelength region close to the excitation b) Second-order Stokes scattering on optical grating of the instrument appears at double excitation wavelength, b) Raman scattering originates from the inelastic scattering of excitation light by molecular vibrations of the solvent or other components in the sample, thus being strongly dependent on a excitation wavelength, solvent and titrant. If overlapping with ligand spectrum, careful spectral interpretation based on the use of solvent blanks, varying excitation wavelengths and appropriate baseline corrections are necessary; c) Light scattering arising from ligand and/or DNA aggregates can significantly distort fluorescence measurements, since it increases turbidity in the sample, leading to enhanced Rayleigh scattering. Detecting aggregation can be achieved by monitoring increase in absorbance baseline, or even simply by shining a laser pointer beam through the sample and observing whether the beam path becomes visible in the solution (Tyndall effect).

Presence of trace impurities in the samples or on the glassware: Impurities in the glassware can be detected by collecting fluorescence spectrum under the same set of conditions for a system containing all components except the dye (the ligand). An impurity in the ligand can usually be detected by examining normalized excitation and emission spectra of the ligand obtained by exciting, or detecting fluorescence at different wavelengths. If the spectra cannot be superimposed, it usually indicates the presence of impurity. Also, excellent overlap of excitation spectrum with UV-Vis spectrum of a ligand is expected.

Ligand-aggregation should be checked by performing UV–Vis and fluorimetric (if applicable) concentration-dependence experiments. A linear Beer–Lambert law response (absorbance vs. concentration) confirms monomeric behavior in the working range. For chiral ligands, circular dichroism spectra (details in section Circular Dichroism (CD) Spectroscopy) at different concentrations can be collected, whereby aggregating ligands could form chiral aggregates with a characteristic exciton-coupled CD spectrum, which is, by the way, diagnostic of the supramolecular chirality.[47,48] Strong changes in UV–Vis spectra of ligands upon heating, which are reversible upon cooling, additionally support aggregation, whereby aggregates are commonly disrupted proportionally to the temperature increase (although there are opposite examples, temperature-induced aggregation of large aromatic compounds[49]. Heating-dependent changes of fluorescence spectra should be taken with caution, since fluorophore emission by itself could be highly temperature sensitive.[41]

DNA/RNA (HOSTS)

Commercial nucleic acids are typically sold as lyophilized fibers, often in sodium salt form, and should be stored strictly according to the manufacturer's instructions. Synthetic DNA / RNA sequences—especially defined duplexes and homopolymers—are preferred for structural binding studies due to their folding uniformity (in well-defined helical secondary structure, see Table 1) and high reproducibility.

The DNA / RNA dissolving should be done strictly as defined by producer, in buffers of appropriate ionic strength. Namely, one of the most common mistakes is use of incorrect conditions, which affect folding and spectroscopic profiles - for instance use of low ionic strength buffer or even pure water, giving only partially folded double strand DNA / RNA. Solid sample DNA / RNA dissolution is slow and can take hours at room

Table 1. The most common secondary structures of ds-DNA/RNA and relevant groove widths and depths parameters. Note the drastic changes accompanied with an A-to-B DNA helix transition.[50]

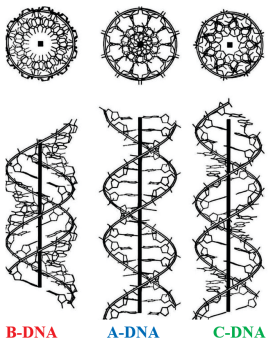

Structure type	Groove width		Groove depth	
	major	minor	major	minor
B-DNA	**11.7**	**5.7**	**8.5**	**7.5**
$(dGdC)_n$	13.5	9.5	10.0	7.2
(dAdT)n	11.2	6.3	–	–
A-DNA	**2.7**	**11.0**	**13.5**	**2.8**
A_nU_n RNA	3.8	10.9	–	–
C-DNA	**10.5**	**4.8**	**7.5**	**7.9**
$D(A)_nd(T)_n$	11.4	3.3	–	–

temperature, or even overnight – otherwise there is a risk of strongly non-homogenous stock solution, which compromises the accuracy and reproducibility of subsequent titration experiments. Natural DNAs like *calf thymus* DNA (ct–DNA) and other, tend to be long and consequently upon addition of buffer very viscous, thus hampering accurate uptake of small volumes with pipette, and thus being impractical for titrations. Sonication of such gel–like DNA solution using a standard bio-compatible probe in short pulses (up to 5 seconds each, with cooling intervals to prevent overheating and denaturation), followed by filtration through sterile 0.45 µm filters, significantly reduces viscosity and produces more uniform DNA fragments (< 100 base pairs), enhancing pipetting precision and data consistency. Similarly, overly concentrated or guanine–rich DNA solutions risk gelation, which hampers accurate aliquot uptake by pipette; to prevent this risk recommended DNA concentration would be in the c = 0.001–0.01 M range.

Concentration: Determination of the DNA concentration is commonly done by application of molar absorption coefficients provided by the producer or by literature data. It is of utmost importance to understand whether by this procedure c(DNA) is defined as c(bases) (equal to c(phosphates) in older references); or as c(basepairs) or for short oligonucleotides as c(folded oligo). If DNA/RNA samples are prepared by annealing from single stranded (ss)oligonucleotides, literature-verified procedures of annealing should be performed (most common is heating to 95°C, and slow cooling by 1 °C min^{-1} to room temperature) and folding quality checked by CD spectroscopy (Figure 1)[31,33] and thermal denaturation experiments (latter not possible for long GC-rich sequences due to denaturation temperatures > 100 °C).[35]

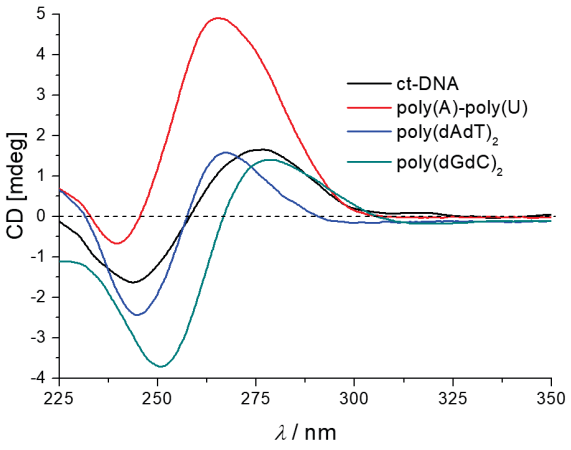

Figure 1. CD spectrum of some commonly used double-stranded polynucleotides at c = 2 × 10^{-5} M in sodium cacodylate buffer at pH 7.0, I = 0.05 M.

METHODS

Small molecule (ligand)/DNA non-covalent interactions are often quite complex, and this guide outlines four commonly used techniques to characterize complexes formed between small molecules and DNA:

Spectrophotometric (UV-Vis or fluorimetric) Titrations
Circular and Linear Dichroism (CD) Spectroscopy
Thermal Denaturation of DNA (Thermal denaturation Curves)
Indicator displacement assay (IDA) relying on techniques described in Spectrophotometric titrations and Circular and Linear Dichroism Spectroscopy

A particular advantages of these methods are: all can be performed in very similar, biorelevant conditions (buffered aqueous solutions of pH 5–8, concentration of ligand and DNA within nM–100 µM range). The equipment is cheap, easily available, and universal: common quartz cuvettes of usually 1 cm pathlength, automatic pipettes, common set of buffers. Also, experiments are relatively fast (0.5–2 h), some can be run in multiplets, and processing, as well as presentation of obtained data, is straightforward. Simultaneous running of several techniques on the same sample is sometimes possible, method sensitivity and sample concentration or volume can be optimised, aiming toward usage of low amounts of expensive DNA samples.

Spectrophotometric (UV-Vis or Fluorimetric) Titrations

UV–Vis and fluorescence spectroscopy are the most common methods for determination of the binding affinity between ligand and DNA, ligand / DNA stoichiometry (for long polynucleotides Scatchard ratio n = [bound ligand] / [DNA] – see the chapter Processing of titration data, and dominant binding site(s) on DNA (intercalation, groove binding, etc.). Other methods, like FR-IR, Raman (SERS), NMR, etc. can also be used for titrations, but usually lack sensitivity or are rather slow.

The dilution effect during spectrometric titrations is a critical factor that must be carefully addressed to ensure accurate data interpretation. This effect arises because the incremental addition of ligand or DNA stock solutions increases the total volume in the cuvette, causing changes in the concentrations of all components. Ignoring this dilution can lead to erroneous binding isotherms and affinity estimates. To mitigate this, dilution can either be accounted for during data processing by mathematically correcting the measured absorbance or fluorescence values according to the changing volume, or it can be minimized experimentally by using highly concentrated stocks and adding small aliquots to keep volume changes negligible. Setting up the experiment

with precise volumetric control and documenting the exact volumes added allows correction of concentration values post-measurement. Some protocols also include parallel control titrations where buffer is added instead of ligand to quantify purely dilution-related spectral changes, which are then subtracted from ligand titration data. Implementing either or both of these approaches helps to avoid artifacts and improve the reliability of binding parameters derived from spectrometric titrations.

UV-Vis Titrations: Advantages, Disadvantages, and Specific Information

The use of UV–Vis titrations depends on the ligand's light absorption above 300 nm, which is necessary to avoid overlap with the strong absorbance of DNA. Their applicability is largely determined by the ligand molar absorption coefficient (ε). For instance, only a limited number of small molecules possess sufficiently strong absorbance at micromolar concentrations, thus, titrations typically require ligand concentrations above 10 μM or the use of extended optical path lengths. Even fewer molecules exhibit absorption maxima above 300 nm that are sensitive to microenvironmental changes, such as solvatochromic compounds, aromatics involved in stacking interactions, or tautomeric species. These molecules can show pronounced spectral changes upon DNA binding, including strong maxima shifts and isosbestic points, which is advantageous for reliable data analysis.

Thus, UV-Vis titrations are generally of limited sensitivity, but nevertheless can yield important information about the nature of ligand/DNA complex: the most common changes are hypochromic effects suggesting interaction of ligand and DNA molecular orbitals. Some ligands show also strong bathochromic shifts (> +20 nm) pointing toward aromatic stacking interactions, either as a consequence of intercalation into DNA, or ligand aggregation.[51] In such cases appearance of isosbestic point strongly supports only one type of binding mode, at variance to systematic deviation. In some cases, specific changes in UV-Vis spectra between aggregated and non-aggregated ligand (Section Ligands (Small Molecules)) can also be seen upon DNA titrations, strongly supporting aggregate involvement, either in the starting ligand solution or aggregation within the DNA binding site.[52] In general, quite often changes are observed at excess of ligand over DNA as a consequence of non-specific agglomeration along polyanionic DNA-backbone and thus, UV-Vis titrations rarely allow collection > 10 data points for single ligand/DNA-binding site dominant binding mode. Therefore, all data should be considered with caution and used in concomitance with the results of other methods.

Fluorimetric Titrations: Advantages, Disadvantages, Specific Information

This method is restricted to ligand chromophores that are either fluorescent in aqueous solution or, even more convenient, become emissive upon binding to DNA.[53] Well-known fluorescence signal sensitivity[41] allows fluorimetric titrations at much lower concentrations (commonly between nM and μM concentrations) of a ligand and DNA in comparison to UV-Vis titrations, and instrument possibilities enable fine tuning of the titration conditions, essential for detailed study of particular conditions, and collection of large number of data points.

However, fluorescence is prone to numerous artefacts (see section Ligands (Small Molecules) and Ref. [41]) and should be carefully planned and analysed. The fluorimeters do not have automatic subtraction of a baseline (common for UV–Vis spectrophotometry) but measuring a buffer spectrum under planned experimental conditions is advisable, because it will reveal Rayleigh, second order Stokes and Raman scattering effects, as well as eventual presence of highly emissive impurities (originating from contaminated buffer, glassware, cuvettes,…). Particularly, excitation wavelength should be carefully chosen and the total absorbance of the sample at the highest c(DNA) should be kept $A < 0.1$ to avoid the possible inner filter effect.[41] The signals originating from aforementioned scattering effects should be taken into account, since they can all change with the addition of DNA and produce false titration curves.

DNA-induced ligand emission can change in many different ways: by hypso- or bathochromic shifts, emission quenching or emission increase, appearance or disappearance of ligand-aggregate emission. Even in cases when the emission spectrum is only marginally changed, advanced techniques can characterise ligand/DNA complexation;[41] for instance, change in fluorescence decay times or fluorescence anisotropy (when a small ligand is bound to very large DNA). Describing all possible changes and their relation to the type of ligand / DNA complex is exceedingly complicated,[41] thus, for the simplicity of this multimethod tutorial, only the most common changes are commented.

Generally, any type of emission change cannot be correlated to any particular binding mode of ligand to DNA. However, in concurrence with other methods, fluorescence change can support indications. For instance, if DNA addition induces the appearance of emission attributed to ligand-aggregate (previously established in section Ligands (Small Molecules) intercalation between DNA basepairs is highly unlikely.

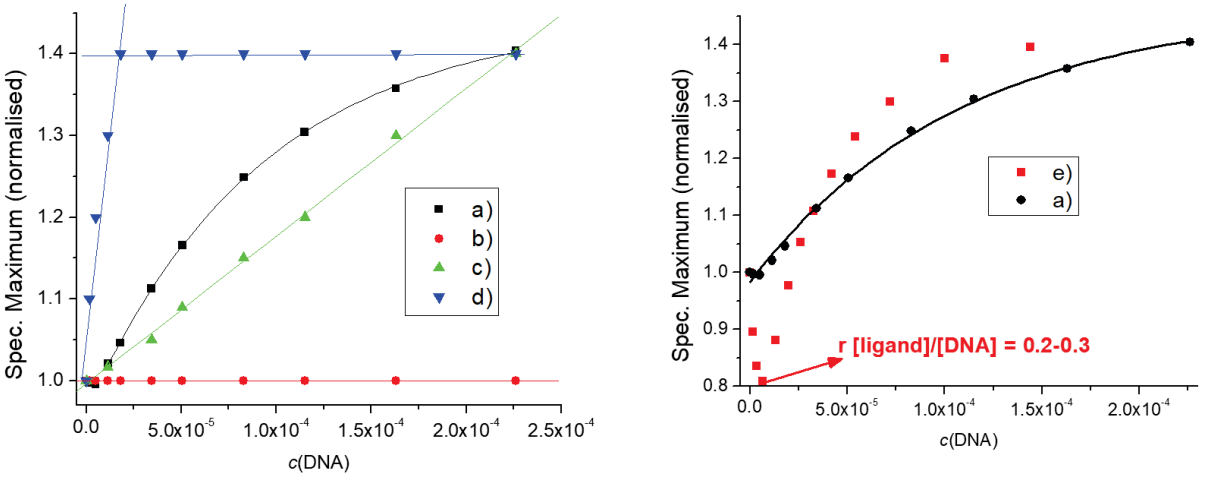

Figure 2. LEFT: The most common types of preliminary titration data. RIGHT: comparison of titration at common ionic strength (e, ■) buffer pH = 7.0, I = 0.015 M, and same sample titration upon addition of 0.1 M NaCl (a, ●).

a) LEFTa: titration data well-fitting to 1st exponential eq. (in Scatchard eq. $c = n \cdot c_0(\text{titrand}) \cdot K_s$ within the 1–10 range), as expected for a simple ligand/DNA complex with one dominant binding mode. Can nicely be fitted to the Scatchard eq. to obtain binding parameters (Section 3.1.3), a collection of the > 10 titration points within the most curved range (20–80 % of complex formed) is recommended.

b) LEFTb: negligible spectral change (> 1 % of signal intensity) even up to 100-fold excess of DNA (usually reaching 0.1 mM DNA): the most probable explanation: method is not sensitive to ligand binding to DNA or there is no biorelevant ligand / DNA interaction.

c) LEFTc: spectral change proportional to c(DNA) as far as 100-fold excess of DNA (usually reaching 0.1 mM DNA): weak binding interaction, not possible to accurately fit to Scatchard eq., thus suggesting $K_s < 10^4$ M^{-1}.

d) LEFTd: measurable change only upon several starting additions (usually changing linearly with c(DNA) and ending at r = [ligand / DNA] =0.5–0.1), followed by no further changes: suggests high binding constant $K_s >> 1 / c$(ligand). Either c(ligand) should be decreased by at least one order of magnitude, or, alternatively, an increased optical path in UV–Vis titration, a more sensitive method, or instrument is sought.

e) RIGHT: Within titration course spectral changes in opposite direction (e, ■), with the breakpoint usually close to r = [ligand / DNA] = 0.3–0.1: at least two different binding modes are present, commonly one at excess of ligand originating to ligand aggregation within DNA binding site, and changes at excess of DNA attributed to single ligand molecule binding to DNA binding sites. Such data set does not allow a simple determination of binding affinity(es). In some cases, decreasing c(ligand) by an order of magnitude and starting titration at an excess of DNA over ligand can yield data for accurate determination of the binding constant to a single binding site. Also, sometimes an increase of ionic strength in solution by e.g. increasing of c(NaCl) for 0.1 M, efficiently suppresses contribution of ligand / DNA electrostatic interactions, thus leaving one dominant type of binding mode.[55]

STARTING PROCEDURE

Starting procedure involves preparation of ligand aqueous buffered solution (taking care that other solvents from ligand or DNA stock solution do not exceed biorelevant concentration) in quartz cuvette (1 cm path length) according to procedures in section 2.1.1. and titrating with increasing amounts of DNA prepared in the same buffer. Commonly, preliminary titration is started by adding equimolar c(DNA) in respect to c(ligand) and proceeds up to 100-fold excess. Spectra are recorded after each addition, taking care that measurable spectral change is observed (larger than the double error of the instrument). For the starting several additions, for each spectrum should be collected several times (usually at 10 sec, 1 min, 2 min, 5 min interval), to check for the incubation time necessary to achieve thermodynamic equilibrium. Namely, the time necessary for a ligand molecules to achieve thermodynamic equilibrium upon binding to DNA can vary from seconds to days (e.g. for threading inetercalators),[9,10,54] most commonly averaging around 1–2 min.

COLLECTION OF THE OPTIMAL TITRATION DATA SET

Inspection of preliminary titration data (section Starting procedure) can reveal several different patterns, each

leading to different conclusions (Figure 2), based on which further action is taken:

PROCESSING OF TITRATION DATA TO DETERMINE BINDING CONSTANTS (K_s) AND STOICHIOMETRIES (SCATCHARD RATIO n = [bound ligand] / [DNA])

A comprehensive and succinct review evaluating DNA binding constants through fluorescence titration spectroscopy, in detail describing way for calculating small molecule binding affinities toward DNA, particularly for fluorogenic ligands, has recently been published.[34]. Complementary descriptions of spectrophotometric titration methods—highlighting their strengths in real-time UV–Vis or CD monitoring of hypochromic shifts and limitations such as interference from absorbing species—along with their integration with isothermal titration calorimetry (ITC), provide deeper insights into nuanced variations in binding thermodynamics and stoichiometry. Further, additional description of characteristics and limitations of spectrophotometric titration methods, as well as combination with microcalorimetric methods, can give additional information about fine differences in binding affinity.[56]

Multivariate spectroscopic measurements allow for reliable determination of stability constants when several criteria are met.[57] These include a reproducible signal–concentration relationship described by a model with parameters that remain constant throughout the experiment (Beer–Lambert law), and the validity of spectral independence among the species present in the reaction mixture. In the case of DNA-binding molecules, multivariate data analysis using the Scatchard equation for equilibrium concentrations calculation yields values for the binding constant and the average number of nucleotides occupied per bound molecule. The molar spectra of spectrally active species are also obtained through data fitting.

Derivation of Scatchard Equation

Scatchard equation is derived from a model where a ligand (L) binds to macromolecule (M) with n identical and independent binding sites.

$$M + nL \rightleftarrows ML_n \tag{1.1}$$

In the case of DNA, the binding sites are represented by individual nucleotides, and n denotes the number of ligands bound per nucleotide. When a ligand occupies more than one nucleotide, n is less than 1, and 1 / n can be interpreted as the average number of nucleotides occupied by a single bound ligand. In this model, the mass balance equations are extended by the factor n, which converts the concentration of DNA nucleotides into the concentration of binding sites:

$$n \cdot c(\text{nucleotides}) = n \cdot [\text{free nucleotides}] + [\text{ML}] \tag{1.2}$$

$$c(\text{L}) = [\text{L}] + K \cdot [\text{L}] \cdot (n \cdot [\text{free} - \text{nucleotides}]) \tag{1.3}$$

Stability constant for the equilibrium of the binding to one independent site is:

$$K = \frac{[\text{ML}]}{(n \cdot [\text{free} - \text{nucleotides}])[\text{L}]} = \frac{[\text{ML}]}{(n \cdot c(\text{nucleotides}) - [\text{ML}])[\text{L}]} \tag{1.4}$$

The fractional saturation r is given by the equation:

$$r = \frac{[\text{ML}]}{c(\text{nucleotides})} \tag{1.5}$$

If [ML] in the [Eq. (1.4)] is substituted by equation above the following expression is obtained:

$$K = \frac{r \cdot cn(\text{nucleotides})}{(n \cdot c(\text{nucleotides}) - r \cdot c(\text{nucleotides}))[\text{L}]} = \frac{r}{(n - r)[\text{L}]} \tag{1.6}$$

This expression is often linearized to the form:

$$\frac{r}{[\text{L}]} = K(n - r) = -Kr + Kn \tag{1.7}$$

where the left-hand side fraction is plotted against r. The slope equals to $-K$ and the number of binding sites n is determined from the intercept.

Changes in Absorbance or Emission Intensity Plotted Against DNA Concentration

In the preliminary analysis of the obtained spectra, several corrections can be made to facilitate the detection of the binding process. These include the simple summation of the spectra of the reactants, scaled to their analytical (total) concentrations in the reaction mixture. If the resulting spectrum differs in shape and/or intensity from the observed spectrum, this is a strong indicator that binding is taking place. The true stoichiometry of the formed complexes can be assessed by plotting single-wavelength values against the titrant/titrand molar ratio, after correcting for dilution effects. In some cases, the titrant may absorb at the chosen wavelength, resulting in signal

changes that resemble a weak binding event. To resolve this, the titrant signal at the chosen wavelength can be subtracted. If the resulting plot shows constant values of the measured spectroscopic quantity, then no binding occurs—or complexation does not induce changes in the spectra of the reaction participants. The Job plot is a classical analytical technique used to determine the stoichiometry of a complex formed between two interacting species, typically a ligand and a metal ion, or a protein and a nucleic acid, etc. The method is based on preparing a series of solutions in which the total molar concentration of the two interacting components remains constant, but their mole fractions vary systematically. For each mixture, a measurable property that reflects complex formation (such as absorbance, fluorescence, or chemical shift) is recorded. The observed signal is then plotted against the mole fraction of one component. The extreme of the Job plot curve corresponds to the stoichiometric ratio of the components in the complex. The Job plot is limited to complexes of moderate to high stability and is used mainly for stoichiometry determination. For these reasons the method is being replaced by systematical data fitting and testing of all reasonable binding models.[58,59]

Recommended Number of Data Points, Focus on Collecting Most of Data in the 20–80 % Of Complex Formation Range

In order to obtain reliable parameter values, careful planning of the experiment is required. In cases where only one form of complex is formed, the value of the stability constant (Figure 3a) and the initial concentration of the titrand (Figure 3b) dictate the shape of the complex formation curve in the distribution diagram. This shape can be easily assessed by calculating a factor *c*:

$$c = n \cdot c_0(\text{titrand}) \cdot K_s \qquad (1.8)$$

where *n* is the average number of binding sites occupied by one guest molecule, c_0(titrand) is the initial titrand concentration and K_s denotes the stability constant. If the value of the factor *c* is between 0.5 and 10, then the shape of the complex formation curve is ideal for reliable stability constant determination. Values above 10 indicate that the binding is too strong in this concentration range, while values below 1 suggest weak complex formation. Factor *c* can be easily adjusted by changing the titrand concentration (Figure 1b), provided that the chosen spectroscopic method yields reliable results in the chosen concentration range. In the case of 1 : 1 competition experiment, changing the concentration range of the experiment does not change the distribution curves of complexes present in reaction mixture if the molar ratio of reactants remains unchanged.

If estimates of stability constant and the average number of occupied binding sites, then the titration can be planned more effectively by performing the titration in the optimal range of complex percentage formation, which is from 20 % to 80 % but can be extended to 0–90 %. Usually, up to 10 titrant additions are enough to obtain good quality data suitable for fitting if the complex percentage formation criteria are met. To further improve experimental conditions, one can carefully choose the volumes of titrant solution in order to uniformly change the percentage formation of formed complexes (Figure 4).[60] This ensures that the total titration range is equally sampled with respect to the spectral property that is proportional to the concentration. In the case of single complex formation, the calculation of the titrant volume is simple:

$$V_{\text{titrant}} = \frac{\alpha\left(100 + n \cdot c_0(\text{titrand}) \cdot K_s \cdot (100 - \alpha)\right) \cdot V_0}{100 \cdot \left(c_0(\text{titrant}) \cdot K_s \cdot (100 - \alpha) - \alpha\right)} \qquad (1.9)$$

where V_{titrant} is the cumulative volume of added titrant solution, α is the percentage formation of the 1 : 1 complex (expressed as a %), K_s is the stability constant of the corresponding complex, c_0(titrand) is the initial concentration of the titrand, and c_0(titrant) denotes the concentration of the titrant stock solution.

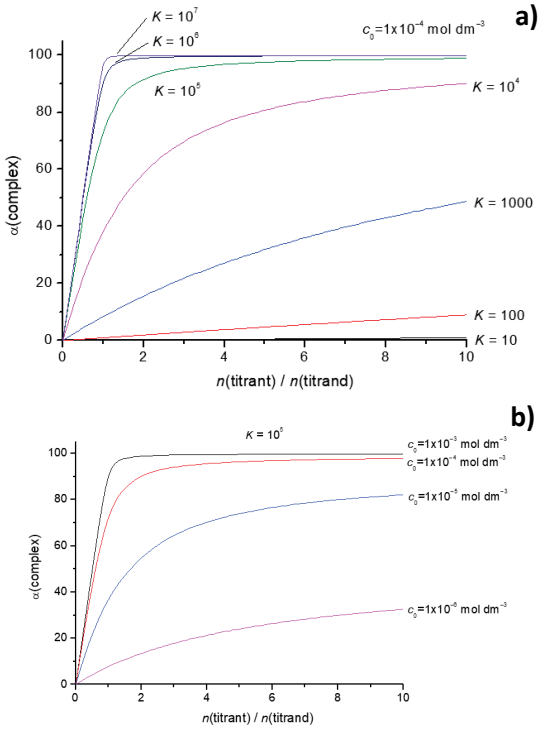

Figure 3. a) Formation curves of 1 : 1 complexes of different thermodynamic stability, b) formation of 1 : 1 complex at different initial concentrations.

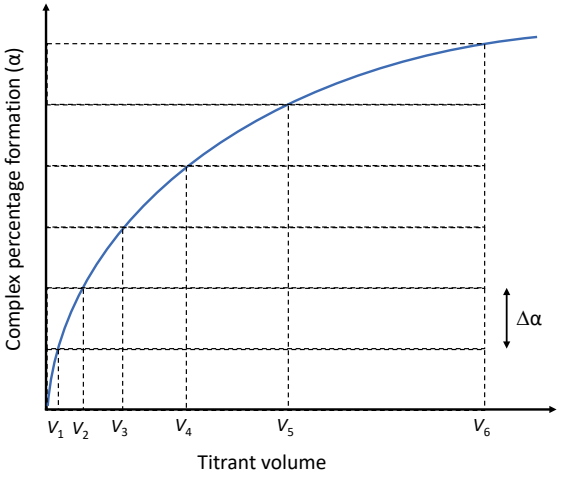

Figure 4. *y*-axis uniform sampling of complex formation curve by adaptive titrant volume selection method.

Non-Linear Least-Squares Fitting of the Binding Isotherm, Advantages of Non-Linear Fitting over Linear Fitting, Advantages of Complete Spectra Processing

The most reliable analysis of the obtained spectra involves non-linear multivariate regression. In this method, multi-wavelength data are used, in contrast to single-wavelength (univariate) data, which are typically applied in preliminary analysis. Fitting of univariate data can lead to erroneous results regarding the values of stability constants and complex stoichiometries,[58,61] especially when paired with model linearization.[62] In multivariate spectrophotometric data analysis, each spectrum recorded during a titration (Figure 5a) is treated as a linear combination of the molar (principal) spectra of spectrally active compounds (Figure 5b), multiplied by their equilibrium concentrations and the optical path length. This relationship can be expressed using the matrix [Eq. (1.10)], where the columns of matrix ***A*** correspond to the recorded spectra, the columns of ***E*** contain the molar spectra of the spectrally active compounds, and the columns of ***C*** contain the equilibrium concentrations of these species for a single spectrum measurement ([Eq. (1.11)]). This is described in more detail in [Eq. (1.12)], where the wavelength dependence of the elements in matrices ***A*** and ***E*** is explicitly shown. When multiple spectra are recorded, [Eq. (1.11)] is extended with additional columns in the absorbance and concentration matrices, as shown in [Eq. (1.13)]. The data fitting algorithm involves finding the optimal values for the stability constant and the average number of binding sites, while the molar (principal) spectra are calculated for each pair of these parameters using matrix multiplication (Scheme 2). For this calculation, the right pseudoinverse of the equilibrium concentration matrix is used. In the case of single complex

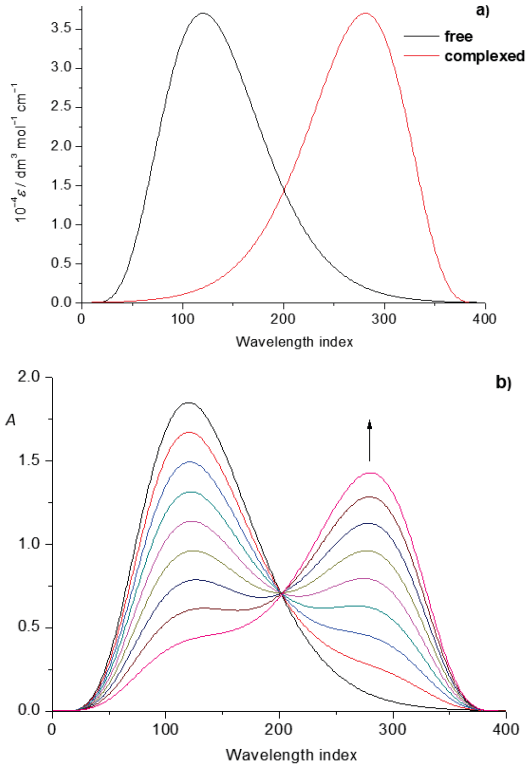

Figure 5. a) Molar spectra of free and complexed spectrally active compound, b) simulated titration data for 1 : 1 complex formation.

formation, the equilibrium concentrations can be calculated directly using the analytical solution derived from the stability constant expression. For more complex systems where ligand dimerization or complexes of multiple stoichiometries are observed, the equilibrium concentrations are obtained numerically by solving the mass balance system of non-linear equations.

$$\boldsymbol{A} = \boldsymbol{E}\,\boldsymbol{C}\,l \tag{1.10}$$

$$\begin{bmatrix} | \\ a \\ | \end{bmatrix} = \begin{bmatrix} | & | & | \\ \varepsilon_1 .. & \varepsilon_j & .. \ \varepsilon_n \\ | & | & | \end{bmatrix} \begin{bmatrix} c_1 \\ . \\ c_j \\ . \\ c_n \end{bmatrix} \cdot l \tag{1.11}$$

$$\begin{bmatrix} A(\lambda_1) \\ . \\ A(\lambda_i) \\ . \\ A(\lambda_m) \end{bmatrix} = \begin{bmatrix} \varepsilon_{1,1}(\lambda_1) \cdots \varepsilon_{1,j}(\lambda_1) \cdots \varepsilon_{1,n}(\lambda_1) \\ . \quad . \quad . \\ \varepsilon_{i,1}(\lambda_i) \cdots \varepsilon_{i,j}(\lambda_i) \cdots \varepsilon_{i,n}(\lambda_i) \\ . \quad . \quad . \\ \varepsilon_{m,1}(\lambda_m) \cdots \varepsilon_{m,j}(\lambda_m) \cdots \varepsilon_{m,n}(\lambda_m) \end{bmatrix} \begin{bmatrix} c_1 \\ . \\ c_j \\ . \\ c_n \end{bmatrix} \cdot l \tag{1.12}$$

$$\begin{bmatrix} | & | & | \\ a_1 \cdot\cdot & a_h & \cdot\cdot a_k \\ | & | & | \end{bmatrix} = \begin{bmatrix} | & | & | \\ \varepsilon_1 \cdot\cdot & \varepsilon_j & \cdot\cdot \varepsilon_n \\ | & | & | \end{bmatrix} \begin{bmatrix} c_{1,1} \cdot\cdot c_{1,h} \cdot\cdot c_{1,k} \\ \cdot \quad \cdot \quad \cdot \\ c_{j,1} \cdot\cdot c_{j,h} \cdot\cdot c_{j,k} \\ \cdot \quad \cdot \quad \cdot \\ c_{n,1} \cdot\cdot c_{n,h} \cdot\cdot c_{n,k} \end{bmatrix} \cdot l \quad (1.13)$$

Although [Eq. (1.10)] to [Eq. (1.13)] are related to spectrophotometric measurements, they can be easily adapted for the analysis of titration data obtained by spectrofluorimetry or circular dichroism. The recorded spectra are stored in the columns of matrix ***A***, the emission or CD molar spectra form the columns of ***E***, the equilibrium concentrations are contained in ***C***, and the optical path length is omitted from the equation. Several tests can be employed to assess the quality of the obtained results. The calculated titration and molar spectra curves should be smooth in the spectral range where reliable values of the spectroscopic signal were recorded. Observed and calculated single-wavelength values should be in agreement, especially in regions with the most pronounced spectral changes. The molar spectra of the reactants should differ in both shape and intensity from those of the formed complexes. Additionally, the set of vectors containing all molar spectra should be linearly independent—that is, none of the vectors should be expressible as a linear combination of the others. Moreover, the molar spectra should be of comparable intensity, within approximately one order of magnitude. If one spectrum dominates this may indicate that the chosen model is unrealistic and that the resulting binding parameters are unreliable. The UV–Vis absorption and emission molar spectra obtained through data fitting should have non-negative values, except in the case of circular dichroism, where ellipticity values may be negative.

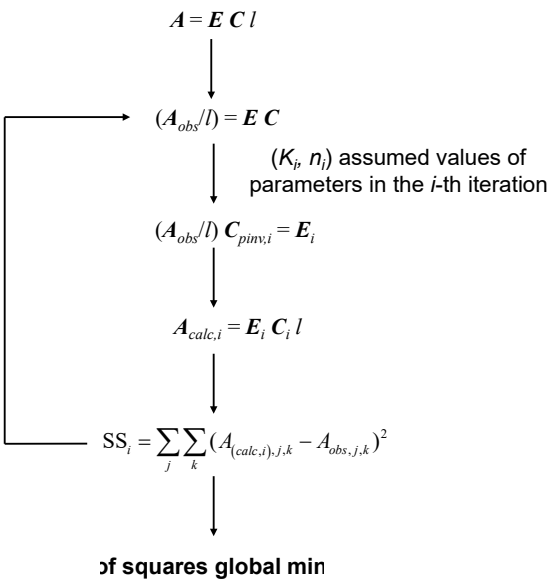

Scheme 2. Algorithm for non-linear fit of multivariate spectroscopic data with response proportional to the equilibrium concentrations of spectrally active compounds.

Data should be fitted by non-linear regression using the original model equation to avoid data transformation through model linearization, which can significantly impact the fitting results. After fitting, additional optimizations should be conducted starting from the values obtained by the initial fit to test for incomplete convergence, or from different initial values to confirm that the global minimum of the sum of squares has been found. Parameters must be tested for correlation. In cases of low to moderate binding, the stability constant and the average number of occupied binding sites are not independent and may change during optimization such that their product remains constant. In such cases, one of the parameters must be fixed to a known or approximate value throughout the optimization. Another way to improve the chances of convergence to realistic values is to include one or more known molar spectra of the reaction participants in the fit. These spectra can be obtained from stock solutions of the reactants or, in the case of strong binding and spectrally inactive titrant molecules, from titration endpoints where nearly all titrand molecules are in the complexed form. If the value of the binding parameter *n* is known—for example, from high-concentration strong-binding experiments—then it can be used to scale the DNA concentration. In this case, the stability constant becomes the only fitting parameter, allowing the use of commercial software such as HyperQuad,[63] Specfit,[57,64] KEV,[65] or ReactLab EQUILIBRIA PRO[66] for multivariate stability constant determination. These programs can be applied to any model with a defined set of equilibria. After defining the stoichiometries of the elementary equilibrium equations, a system of nonlinear mass-balance equations is constructed. This system is usually solved using the Newton–Raphson method to obtain equilibrium concentrations from initial stability constant estimates. In most cases the optimal values of the stability constants are then obtained using the second-order Levenberg–Marquardt optimization method, which identifies the coordinates of the global minimum of the sum of squares. Several difficulties can arise from the use of optimization methods to find the optimal solution, such as convergence to local minima, incomplete convergence, or unreliable determination of parameters. These problems can be mitigated by repeating the optimization from different starting values or by employing an appropriate experimental design.

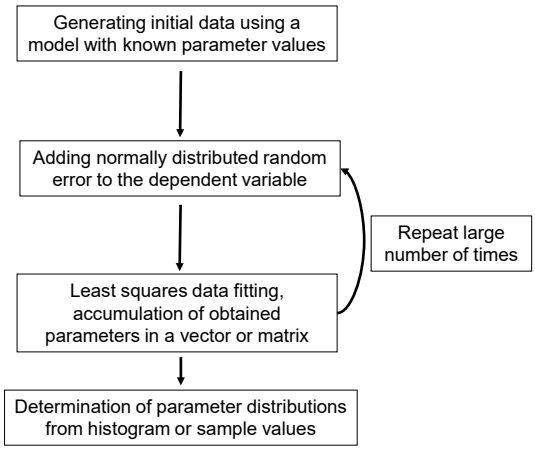

Scheme 3. Monte Carlo algorithm for least squares data fitting.

The uncertainties of the obtained parameter values can be calculated from the fit, and most fitting software provides the standard error of the parameter (standard deviation) upon convergence. This statistic can be used for a quick assessment of the fit quality. A rule of thumb is that the standard deviation of a parameter should not exceed 20 % of its value. A more concise and statistically rigorous method for determining parameter uncertainties is to perform Monte Carlo simulations of the data fitting procedure (Scheme 3). First, the titration data are simulated from the obtained fitting parameters and reaction conditions in the same way as in the optimization algorithm (Figure 6a). Then, a set of random normally distributed error vectors is added to each spectrum to simulate experimental noise (Figure 6b). The data fitting is repeated, resulting in parameter values that differ from the initial ones. This process is iteratively repeated, each time with a new set of random error vectors. The resulting parameter values are accumulated, plotted as histograms (Figure 4c), and their standard deviations are calculated from the sample. This approach directly propagates the uncertainties of the measured spectral response into uncertainties of the model parameters under fixed titration conditions. It can be used both to assess the quality of the obtained parameter values and to plan titration experiments.

Global Fit Procedures, Problems and Advantages

For simultaneous multivariate fitting of spectroscopic titration data, a global fitting procedure can be employed (Figures 7 and 8).[67,68] This approach is useful in cases where binding parameters are correlated or when calculating molar spectra from titrations with low endpoint complex percentage formation. The optimal titration concentration range depends on the spectroscopic method

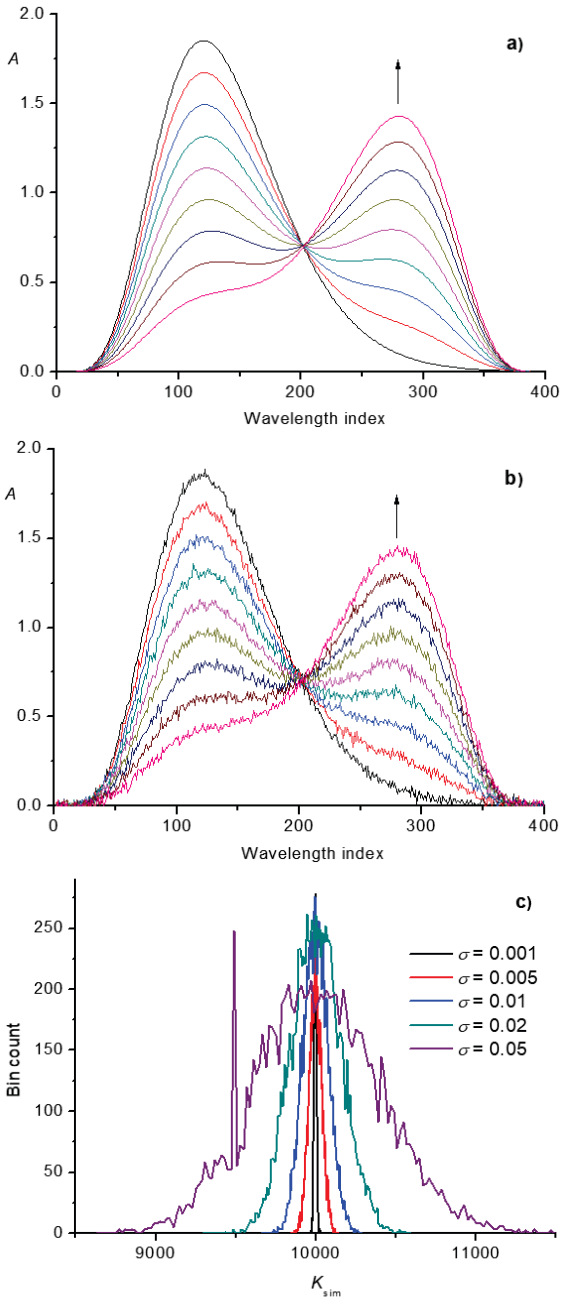

Figure 6. a) Simulated titration spectra for the formation of single type of complex, b) titration spectra with superimposed normally distributed error, c) distributions of stability constant values obtained by Monte Carlo simulations with different standard deviations of superimposed error.

and the response of spectrally active reaction participants. When only a 1 : 1 type of complex is observed, titrations at higher concentrations yield strong binding data, which is optimal for determining the average number of binding

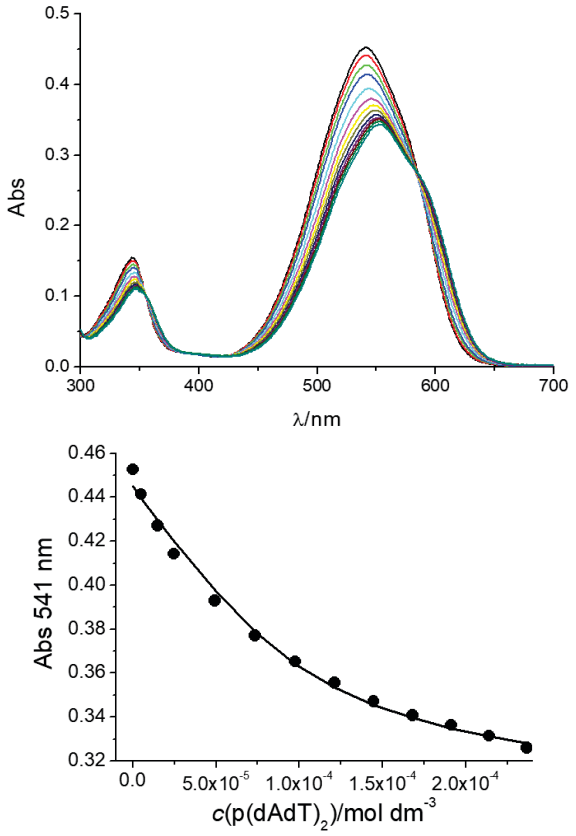

Figure 7. Changes in UV / Vis spectrum of a flavylium dye (c = 1 × 10^{-5} mol dm^{-3}) in the titration with poly dAdT–poly dAdT (LEFT) and dependence of absorbance at λ_{max} = 541 nm on (poly dAdT–poly dAdT), pH 5.0, sodium cacodylate buffer, I = 0.05 mol dm^{-3} (RIGHT). The fitting to the Scatchard eq.[68]

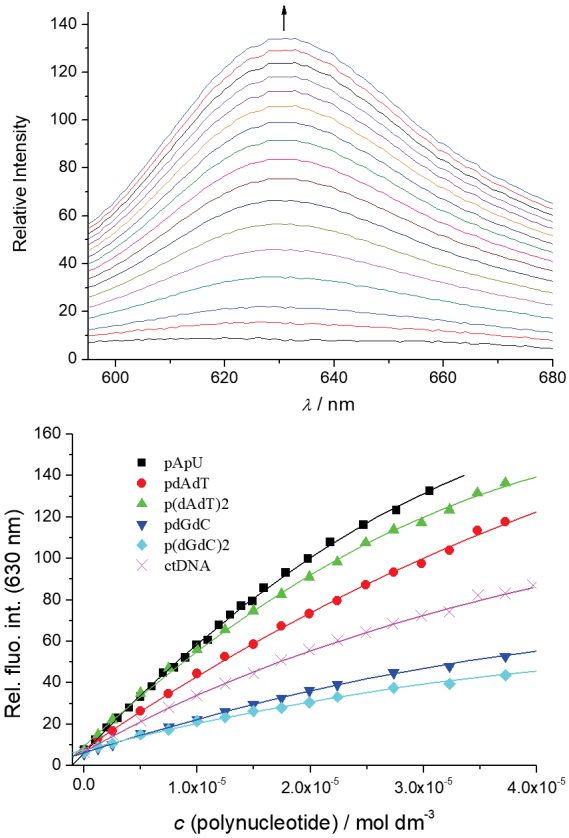

Figure 8. Strong increase of emission intensity of a flavylium dye (c = 1 × 10^{-5} mol dm^{-3}, $\lambda_{exc.}$ = 541 nm) in the titration with poly dAdT–poly dAdT (LEFT) and dependence of relative emission intensity $\lambda_{em.}$ = 630 nm upon the addition of various ds-polynucleotides (sodium cacodylate buffer, pH = 5.0, I = 0.05 mol·dm^{-3}) (RIGHT). Data were fitted by non-linear least square procedure according the Scatchard equation (▬).[68]

sites but is usually inadequate for reliable stability constant determination. Conversely, titrations performed at lower concentrations are more suitable for determining the stability constant, although they are prone to parameter correlation. Combining low- and high-concentration titration data through a global fitting procedure allows for the simultaneous and reliable determination of the complex stability constant and the average number of occupied binding sites. In this procedure, the global sum of squares is minimized by an optimization method in the space defined by the values of the stability constant and the average number of occupied DNA binding sites (Scheme 1). The global sum is equal to the sum of squares corresponding to all experiments included in the fitting procedure. One way to combine data obtained by different methods is to normalize each term in the sum of squares by dividing it by the absolute difference of the physical quantity measured between the first and last spectrum at the wavelength where the maximum change due to complexation is observed. This procedure can be extended to models with multiple complex stoichiometries, as in the fitting of single-method multivariate data.

Prediction of DNA-Ligand Complex Stability by Modern Computational Methods

Predicting stability constants for DNA–ligand complexes via machine learning is a promising yet underdeveloped area. There are machine learning tools that can predict the stability of RNA–ligand[69] or DNA–protein complexes,[70] or the docking poses of ligand binding.[71,72] Progress in this field is likely to follow the trends observed in machine-learning predictions of metal–ligand (M–L) complex properties,[73,74] which generally follow two approaches: using features derived from the M–L complex itself, typically from first-principles calculations, or using features

calculated separately from the metal and the ligand. Because the three-dimensional structure of the DNA–ligand complex in aqueous solution is often uncertain, most studies predicting overall stability constants will certainly rely on docking the ligand to DNA using computational software.

PITFALLS IN TITRATION-BASED DNA BINDING STUDIES

While titrations are a powerful tool for quantifying binding affinity and interaction modes, several technical and interpretive issues can affect accuracy and reproducibility. Below are the most common pitfalls to be aware of:

A. Inaccurate Concentration Determination

Problem: DNA and ligand concentrations are critical for reliable binding curves. Errors in quantification (e.g., impure oligonucleotides or inaccurate absorption coefficients) can distort binding constants and ligand / DNA stoichiometries.

Solution: Use high-quality, HPLC-purified oligonucleotides; check DNA concentration by absorbance at exact conditions (buffer, ionic strength, pH) using sequence-specific wavelength and molar absorption coefficients. Measure ligand absorbance directly in buffer and validate with the known standard. UV–Vis spectrum (section Ligands (Small Molecules)).

B. Buffer Mismatch and pH Drift

Problem: Different buffers for DNA and ligand stock solutions can cause artefacts (e.g., absorbance / emission unexpected / inexplicable changes or precipitation). pH-sensitive ligands may change p*K* upon interaction with DNA.

Solution: Prepare all stock solutions in the same buffer. Compare results with pH-dependent UV-Vis spectra of a ligand (section Ligands (Small Molecules)), especially when working near the pK_a of the ligand.

C. Ligand Self-Aggregation or Fluorescence Quenching

Problem: At the ligand excess over DNA, some small molecules self-aggregate, causing changes in spectral properties.

Solution: Compare with the aggregation properties of a ligand (section Ligands (Small Molecules)).

D. Inner Filter Effect (Fluorescence Titrations)

Problem: High absorbance at the excitation or emission wavelengths leads to signal attenuation, giving misleading results.

Solution: Keep total sample absorbance at the end of titration with DNA below 0.1 at the excitation wavelength. If dilution of a sample is not applicable, consider a shorter optical pathway, or approaches to avoid problem[42] or use Inner Filter correction formulas.[43]

E. Poor Mixing and Sample Inhomogeneity

Problem: Incomplete mixing can cause sample variability and inconsistent spectra.

Solution: Check DNA stock solution for uneven viscosity or gel particles (see section DNA/RNA (Hosts)). Mix gently but thoroughly after each addition (e.g., pipette up and down 3–5 times or use magnetic stirring for cuvettes).

F. Incorrect Binding Model Fitting

Problem: Applying a simple 1 : 1 binding model to complex binding interactions (e.g., cooperative binding, multiple modes) leads to poor fits and inaccurate K_s values.

Solution: Inspect residuals of the fit, try multivariate fitting models (e.g., Specfit / HyperQuad multiple-site models), and validate complete titration range or partial titration range with independent methods (e.g., CD or thermal denaturation assays), eventually by application of GlobalFit procedures.

G. Dilution Effects

Problem: Large-volume titrations can change total concentrations significantly, especially at low DNA or ligand levels.

Solution: Either correct for dilution mathematically or use a reverse titration format (fixed DNA, increasing ligand) with minimal volume change.

H. Temperature Variability

Problem: Binding affinities are temperature-dependent, therefore ambient temperature drift during titrations can cause inconsistent readings. Also, fluorescence of some ligands is extremely temperature sensitive, as noted in section DNA/RNA (Hosts).[41]

Solution: Perform titrations in a temperature-controlled room or use a cuvette holder with thermal regulation.

I. Over-Interpretation of Signal Changes

Problem: Not all signal changes equate to specific binding; some may arise from nonspecific interactions or ligand rearrangement.

Solution: Confirm results with complementary methods such as thermal denaturation, CD spectroscopy, or NMR / ITC, and interpret spectral changes in a structurally logical context (for instance, bulky ligands cannot intercalate, neutral ligands cannot base their affinity on interactions with polyanionic DNA backbone, etc).

Circular Dichroism (CD) Spectroscopy

Chirality is a property possessed by the majority of natural compounds, characterized by the lack of superimposable mirror images, which exist in the form of enantiomers. Hence, for monitoring such molecules, a sensitive spectroscopic method is much needed. Circular dichroism (CD) is a polarization spectroscopy used to study the differences in the absorption of left- and right-handed circularly polarized light by a sample containing chiral molecules.[75,76] It provides valuable insight into the structural features and conformational changes of the studied compounds, due to various alterations in the chiral

environment around chromophores, which can influence the CD spectrum of the studied compound.

The double-stranded helix of DNA has a distinct chirality due to the spatial arrangement of the bases around the helical axis. Consequently, the CD spectrum strongly depends on the DNA secondary structure as well as used experimental conditions.[76,77] This can be employed for checking the quality of DNA samples (see section DNA/RNA (Hosts)).

Moreover, small achiral molecules (ligands), do not possess CD spectrum, but upon binding to DNA can change the structure of DNA (consequently altering its CD spectrum). Moreover, if ligand molecule is dominantly uniformly oriented in respect to DNA chiral axis, it could acquire induced (I)CD spectrum within the range of ligand UV–Vis absorption spectrum. The sign, shape and intensity of such ICD bands can be used for analysis of ligand orientation within DNA binding site and thus, help in determination of binding mode.

For this reason, several step-by-step guides have been published on the use of CD / LD spectropolarimetry to monitor DNA conformational changes upon ligand binding,[31,32] as well as a comparative overview outlining how CD and LD results can be interpreted with respect to the most common ligand–DNA binding modes.[33] In the present work, only the most essential facts related to other methods will be summarized, while further details can be found in the aforementioned references.

In the context of studying non-covalent DNA / RNA–small molecule complexes, CD spectra can often be divided into two wavelength-dependent ranges (Figure 9).

The Wavelength Range Between 200–300 nm

The wavelength range between 200–300 nm is characteristic of DNA, the most common CD bands for right-handed DNA being a strongly negative band at about 245 nm and a strongly positive band within 265–290 nm range. It is essential to check whether the UV spectrum of a ligand absorbs significantly within this range, and strongly advised in such cases to plot the ligand UV spectrum above CD spectra results. If the contribution of ligand absorption is weak or negligible, changes of DNA bands upon ligand binding can be attributed to the change of DNA helix chirality. The most common change is decrease of CD-band intensity, usually attributed to ligand-induced unwinding / kinking / disruption of DNA helical secondary structure. However, if ligand absorbs light in the mentioned range, detected CD changes cannot be assigned to polynucleotide only, due to the co–presence of several CD–active species: intrinsic and ligand-changed CD spectrum of DNA / RNA and the induced CD (ICD) signal of the ligand. In combination with other methods, particularly titration results (section Spectrophotometric (UV-Vis or fluorimetric) Titrations), sometimes deconvolution of spectra is possible by using multivariate analysis of complete spectra, allowing analysis of changes in DNA chirality.

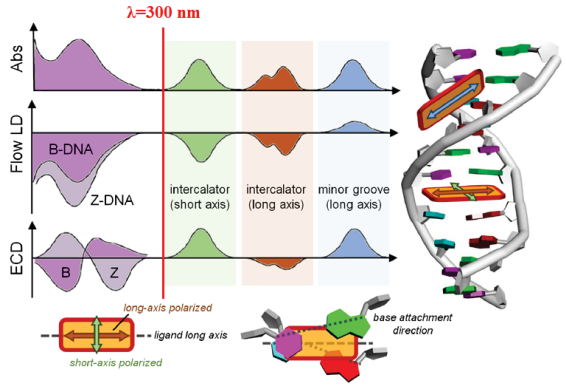

Figure 9. Characteristic bands in the CD or LD spectrum. Obtained by permission and modified from.[33]

Wavelength Range Above 300 nm

Wavelength range > 300 nm is attributed to the light absorption of the ligand only, thus giving, in the case of an achiral ligand, highly informative signals. Appearance of isodichronic points strongly supports formation of only one dominant type of ligand / DNA complex, and observed spectrum could be directly correlated to the binding mode and the geometry of the ligand / DNA complex (Figure 9, details in Ref. [33]).

The scenario is not so straightforward with chiral ligands, which have an intrinsic CD signal, so the difference in the CD spectrum caused by ligand/DNA binding is complex for the same reason mentioned above for the system described in section The Wavelength Range Between 200 and 300 nm, and could also only be deconvoluted by the mentioned multivariate techniques.

PROCEDURES (CD SPECTROSCOPY)

The results described in sections Starting procedures, Collection of the optimal titration data set, and Processing of titration data to determine binding constants (K_s) and stoichiometries (Scatchard ratio n = [bound ligand]/[DNA]) are essential for adequate planning of CD experiments, particularly the shape of the ligand UV–Vis spectrum, information about one dominant or several distinguishable ligand / DNA complexes, binding constants, and binding stoichiometry (Scatchard ratio n = [bound ligand] / [DNA]). Furthermore, experimental conditions and equipment are usually very similar as used in section Spectrophotometric titrations, thus in many cases the same sample can be measured. For instance, ligand sample in 5–10 μM concentration can be measured by all three instruments: UV–Vis, CD, and fluorescence spectrophotometer.

It should be stressed that common CD titration is performed in opposite order to UV-Vis or fluorimetric titrations:[31,33] first the CD spectrum of spectroscopically active species (DNA, 10–20 μM) is collected (also used to check DNA helix integrity, as shown in section DNA/RNA (Hosts)), and then aliquots of ligand are added, either in a detailed quantitative titration experiment (allowing binding constant determination, but rather slow)[31] or faster, gathering qualitative information about ligand / DNA structure, collected in molar ratio r[ligand] / [DNA] = 0.05–1.[33,77]

The detailed explanations of the experimental conditions given below can be found in comprehensive tutorials.[7,33]

Practical Binding Experiment/Step by Step Procedure

Pipette 2 mL of buffer into a 1 cm pathlength cuvette (capacity: 3 mL), then record its ECD spectrum. Buffer spectra may show nonzero signals, so always subtract the latest buffer spectrum from subsequent sample scans. Ensure the cuvette remains in the same orientation throughout the experiment.

Add DNA stock solution to the cuvette to achieve a final concentration of 10–40 μM polynucleotide. Record the ECD spectrum and subtract the corresponding buffer spectrum. The baseline above 300 nm should be flat. If it deviates, check for solution turbidity or other issues detailed in Chapter General Considerations in Ligand–DNA/RNA Interaction Studies.

Add ligand stock solution (preferably at mM concentrations) in increments to reach r[ligand] / [polynucleotide] ratios from 0.1 to 1 in steps of 0.1. This ratio range typically reveals all major binding events, as depicted in Figure 2, suitable for detailed analysis. Incubation time before recording each spectrum depends on the binding kinetics; determine this using prior UV / Vis or fluorescence titration experiments. After each addition, subtract the buffer spectrum.

Each ECD spectrum requires 10–20 minutes of acquisition (depending on a scan rate and multiple accumulations). Process and compare spectra during measurement to monitor real-time spectral changes. If the baseline shifts in a wavelength region where neither DNA nor ligand absorbs, immediately investigate for turbidity (see Chapter 2).

Continuously monitor absorbance during measurements. Ensure the sample's total absorbance never exceeds upper limit recommended by instrument producer (typically A = 1.5 – 2.0).

RESULTS (CD SPECTROSCOPY)

In analyses of induced CD (ICD) bands, aside from characteristic sign (negative or positive) also expressions as "weak" or "strong" are also used. Latter are of a relative nature and refer to the intensity of DNA bands.

Here are listed the most common CD results for a simple system of achiral ligand/DNA complex (Figure 9):

i) Intercalative ligand / DNA binding usually yields at λ > 300 nm a weak negative ICD signal (additionally supported by ILD band, Fig. 3). Occasionally, intercalators yield only weak or negligible ICD signals due to a non-parallel orientation of their transition vector relative to adjacent base-pair axes. The ICD(ILD) response non-linearly changing upon titration of DNA with ligand, reaching the saturation approximately at the ratio r[ligand] / [DNA] = 0.2–0.3, which should correlate well with calculated Scatchard ratio n = [bound ligand] / [DNA]. Further ligand additions, at r > 0.3, yield an excess of ligand over DNA binding sites, and in some cases can induce the appearance of novel ICD bands, attributed to ligand aggregation along DNA. Within a 200–300 nm range, a significant decrease of DNA bands intensity is expected, but only in the range where ligand absorbance is negligible (see section The Wavelength Range Between 200–300 nm).

ii) Ligand binding into DNA groove (mostly minor groove of B-helical DNA, or major groove of A-helical DNA, due to narrow and deep size of grooves, Table 1) commonly causes a strong positive ICD band (Figure 9). The ICD(ILD) response is non-linearly changing upon titration of DNA with ligand, reaching the saturation approximately at the ratio r[ligand] / [DNA] = 0.2–0.4. Quite often at higher ratio r (excess of ligand over DNA) two ligand molecules by aromatic stacking with each other within minor groove form a dimer, and in further adding, ligand molecules sometimes self-organize in oligomers, stretching within DNA groove.

iii) Since both, intercalation and groove binding, can extend at r > 0.3 (sometimes even at r > 0.1) in the secondary binding mode, ligand aggregation along the DNA, it is essential to recognize this event. The dimer / aggregate is commonly characterized by exciton-coupled bisignate ICD bands. Interpretation of the obtained results in respect to aggregate structure and position within DNA is rather difficult due to the many different possible types of aggregates that can be formed, from differently organized dimers[78] to even larger aggregates, such as J– or H–type ones[79] at an additional excess of ligand over DNA.

iv) Absence of any change in CD spectrum upon titration with ligand does not necessarily denote lack of interaction. If several other methods clearly show interaction and biorelevant affinity, the absence of CD response at the same conditions commonly points toward agglomeration of ligand molecules along the outer surface of DNA, with non-uniform orientation in respect to the DNA chiral axis or may indicate a degenerative coupling of transition dipoles, even without aggregation. This is sometimes seen for highly positively charged, flexible

ligands with small aromatic moieties, which tend to wrap around DNA backbone, preserving helical structure (thus no change in CD spectra of DNA) and weak transition moments of aromatic chromophores oriented in many different ways, yielding non-uniform and weak ICD bands, within the signal-to-noise ratio.[33]

v) Major or complete loss of CD spectrum, caused by ligand addition. Such a rare event commonly denotes ligand ability to strongly destabilize DNA secondary structure,[80] and is typically accompanied by a strong decrease of the DNA thermal denaturation point.

Chirality of a ligand complicates interpretation of the results, particularly in a 200–300 nm range, where signals from free species (DNA and ligand) overlap with those of the ligand / DNA complex(es). Even > 300 nm range, the CD spectrum of a free ligand may be altered by interactions with DNA, and eventually overlapped by ICD bands of ligand-chromophore oriented uniformly in respect to DNA chiral axis. Simply subtracting the free ligand spectrum from experimental titration data cannot fully account for these effects and may lead to erroneous conclusions.

An ideal case of collecting enough data points for accurate non-linear fitting[31] and determination of binding constant is rarely possible due to limitations of CD spectropolarimetry. However, if binding constant (K_s) was determined accurately by prior experiments (section Spectrophotometric (UV-Vis or Fluorimetric) Titrations), CD titration data can be analyzed by using multivariate non-linear analysis of commercially available programs (section Processing of titration data to determine binding constants (K_s) and stoichiometries (Scatchard ratio n = [bound ligand]/[DNA])) with known CD spectra of free DNA and free ligand, and by inserting the known K_s value of the ligand / DNA complex. So, the obtained CD spectrum of the fully formed ligand / DNA complex can be compared with CD spectra of the free species to draw general conclusions about changes in chirality and structure.

CD RESULTS CORRELATION WITH OTHER METHODS

The changes in CD spectra of DNA (λ = 200–300 nm range), if not obscured by ligand absorption (section Spectrophotometric (UV-Vis or Fluorimetric) Titrations), represent the changes in DNA secondary structure, giving valuable information about distortions (loss of chirality, typical for some binding modes), or in some cases, chirality increase. The ICD bands at the λ > 300 nm range prove well-defined orientation of a ligand in respect to the DNA chiral axis, in concurrence with other methods (Conclusions, Table 2) strongly supporting particular binding mode (Figure 9). Also, ICD band shape during titration clearly marks the transition from the single ligand molecule dominant binding mode to ligand aggregation, allowing more accurate choice of the range of UV–Vis or fluorimetric titration data for calculation of binding constant (sections Collection of the optimal titration data set and Processing of titration data to determine binding constants (K_s) and stoichiometries (Scatchard ratio n = [bound ligand]/[DNA])).

PITFALLS IN CD TITRATIONS

Although CD spectropolarimetry is indispensable method in determination of ligand / DNA binding modes, it has limitations and pitfalls similar to other spectrophotometries (section Spectrophotometric (UV-Vis or fluorimetric) Titrations), as well as some specific problems for chirooptical methods. The most common pitfalls are listed below:

A. Quality of DNA sample

Problem: improperly or partially folded DNA, as a consequence of poor preparation or impurity (section DNA/RNA (Hosts)), or subsequent denaturation / contamination, directly hampers chiral response and renders all collected data useless.

Solution: For each titration validate the shape and intensity of DNA CD spectrum against known standard. Also take care not to challenge DNA integrity during experiment, for instance by significantly lowering the ionic strength (i.e., upon dilution by ligand solution addition).

B. Baseline increase/change during titration

Problem: An apparent positive drift of the baseline during ligand concentration increase in the cuvette, usually best seen in the long-wavelength range of the spectrum, hampers subtraction of baseline from collected spectra, rendering data useless. This is a clear evidence of precipitation or colloid / aggregate formation in the cuvette, usually also noticed in UV–Vis titrations (section Spectrophotometric (UV-Vis or Fluorimetric) Titrations.

Solution: Decrease DNA concentration, increase number of accumulations of spectrum for enhanced sensitivity and focus on the conditions of excess of DNA over ligand (r < 0.2).

C. Temperature Variability

Problem: Some DNAs have low thermal denaturation points (i.e. AT–DNA oligonucleotides), thus ambient temperature drift during titrations can cause inconsistent readings.

Solution: Perform titrations in a temperature-controlled room or use a cuvette holder with thermal regulation.

D. Misinterpretation of Signals

Problem: Changes in CD spectrum during titration can be very complex, in respect to sign, intensity, signal-coupling, as in detail elaborated in recent tutorials.[33]

Solution: For advanced analysis of complex systems only application of advanced molecular modelling study, if possible coupled with other structure-informative methods (e.g. NMR) can eventually give accurate structure.[81]

E. Unexpected Signals

Problem: CD bands might arise at wavelength range at which neither DNA nor ligand absorb. CD spectropolarimetry is highly sensitive to the particle size, so formation of particles of very uniform diameter (i.e. by ligand-induced DNA condensation in globular shape),[82] will give inexplicable CD band at wavelength proportional to the particle diameter distribution.[83] Such phenomenon is not related to standard chiroptical properties.

Solution: Decrease DNA concentration, increase number of spectrum accumulations for enhanced sensitivity, and focus on the DNA over ligand excess ($r < 0.2$) conditions. If signal persists, it is advisable to refer to a set of methods dealing with DNA condensation (AFM, DLS).

Thermal Denaturation (Thermal denaturation Temperature Shift, ΔT_m)

At variance to methods described in section Spectrophotometric (UV-Vis or fluorimetric) Titrations and partially also in section Circular Dichroism (CD) Spectroscopy, this method monitors primarily intrinsic property of DNA secondary structure, temperature-induced unfolding (common expressions are denaturation, melting) of ds-DNA, G–quadruplex or other poly-stranded DNA forms into ss–DNA constituents. The DNA denaturation point (T_m) presents a temperature at which half of the poly-stranded DNA is unfolded into ss–DNA. Non-covalent binding of small molecules to ds-polynucleotides usually enhances the thermal stability of the ds-helices thus resulting in increased T_m values (positive ΔT_m), although some ligands could also destabilise DNA, which is manifested by negative ΔT_m. Obtained denaturation curves can be very informative about ligand / DNA interactions, observing difference between one dominant binding mode or several coexisting modes, showing saturation of dominant binding sites, which can be correlated to Scatchard ratio n = [bound ligand] / [DNA] (from section Processing of titration data to determine binding constants (K_s) and stoichiometries (Scatchard ratio n = [bound ligand]/[DNA])), as well as with CD results (section Results (CD Spectroscopy) - i)=, and also, some general stabilization effects related to type of binding mode.[35] However, it should be stressed that this method is performed at significantly increased temperature, thus, direct correlation of obtained stabilisation effects cannot be directly correlated to the thermodynamic equilibrium of ligand / DNA interactions at biorelevant conditions (room temperature or 37 °C).

PROCEDURES (THERMAL DENATURATION)

Method is based on the determination of a relative value (ΔT_m) by subtracting the denaturation point of DNA (T_m) alone from that of the ligand / DNA complex. Therefore, it is highly advisable to perform experiment simultaneously with DNA solution and several ligand / DNA solutions differing in ratio r[ligand] / [DNA]. Since during heating the samples may experience unexpected bubbling, precipitation, or other hindrances can occur in only some samples, it is recommended to test simultaneously all samples in duplicates. Such organization of the experiments is possible due to the most common instrument (UV–Vis spectrophotometer with 6–12 cuvettes holder and adequate DNA-denaturation software), and recently also available analogous CD instrument.

For the better comparison with other methods, experiments are usually performed at very similar conditions to UV–Vis or CD titrations (sections Spectrophotometric (UV-Vis or fluorimetric) Titrations or Circular and Linear Dichroism (CD) Spectroscopy), including buffer, ionic strength, concentration of DNA, standard type of quartz cuvette, and eventual traces of other solvents.

DNA Samples Preparation

Take into account that some DNA oligonucleotides (particularly AT-rich) have very low thermal denaturation points, in contrast to GC-polynucleotides, which melt > 100 ºC, and thus cannot be studied by this method. To avoid pipetting errors by adding small aliquots of DNA stock solution to large number of cuvettes, it is advisable to prepare adequate volume of DNA solution (typically 5–20 μM) and distribute it in cuvettes. Alternatively, after aliquots of DNA stock solution are added to all cuvettes, c(DNA) can be determined spectrophotometrically (as per section 2.1.2). The latter approach is advisable when the ligand stock solution is in an organic solvent (i.e. DMSO), from which an aliquot is added to the DNA – in this case exact amount of DMSO has to be added to the free DNA sample.

Ligand Addition

Dependence of ligand UV spectrum on temperature was previously characterised (section Ligands (Small Molecules)), and observed changes should be taken into account. Most ligands do not show significant change at here used concentrations (typically μM range). Upon ligand addition to all DNA samples (commonly r[ligand] / [DNA] = 0.1, 0.2, and 0.3) incubation period determined at section Spectrophotometric (UV-Vis or fluorimetric) Titrations should be taken into account if longer than 10 min.

Instrument Setup

All samples are put in a multicell holder and commonly absorbance at 260 nm (or 295 nm for G–quadruplexes) was monitored from 20 °C to 95 °C, at 0.5 °C intervals, a heating ramp rate of 0.5 °C min^{-1} using a temperature-controlled UV-Vis spectrophotometer. Analogous experiment in CD spectropolarimeter commonly monitors typical DNA bands

(section Circular and Linear Dichroism (CD) Spectroscopy). Such experiment for 12 cuvettes usually takes 1–2h.

However, more recent studies stress additional approaches, which, within marginally longer invested time, offer additional information.[84] The study introduces a method that captures the full UV-visible absorbance spectrum at each temperature point, rather than relying solely on the standard 260 nm absorbance. This approach allows for tracking of thermal denaturation in systems where other wavelengths (e.g., for ligand-bound or noncanonical structures) may be more informative. The method is especially useful for nucleic acid structures complexed with fluorogenic ligands, where traditional absorbance techniques may not adequately capture changes in secondary structure.

RESULTS (THERMAL DENATURATION)

Thermal denaturation temperatures (T_m) were commonly calculated as the inflection point of the of the thermal denaturation curve (Figure 10A), also often presented as a maximum of first derivative (Figure 10B), and the relative value of stabilisation induced by ligand (ΔT_m) by subtracting the denaturation point of DNA (T_m) alone from that of the ligand / DNA complex:

Calculation of Stabilisation:

$$\Delta T_m = T_m(\text{DNA + ligand}) - T_m(\text{DNA alone})$$

Results from at least two independent measurements were compared based on the shape of the denaturation curves, ensuring that differences in hyperchromic shift did not exceed the instrument setup rate of 0.5 °C. Additional comparison criteria included the shape and flatness of the baseline regions before and after the thermal denaturation transition. When the data were consistent within the instrument's error margin, the calculated ΔT_m values were averaged to yield a final ΔT_m value reported with an error of ± 0.5 °C.

Some additional conclusions may be retrieved from the experiments. For instance, monophasic curve (Figure 10, r = 0.1) supports one dominant binding mode and so obtained ΔTm values often increase proportionally with ratio r[ligand] / [DNA] until abrupt binding sites saturation (commonly about r = 0.2–0.3), which can be correlated to calculated Scatchard ratio n = [bound ligand] / [DNA] (from section Processing of titration data to determine binding constants (K_s) and stoichiometries (Scatchard ratio n = [bound ligand]/[DNA])), as well as with CD results (section Results (CD Spectroscopy - i). However, sometimes due to scattering of results around the thermal denaturation curve inflection point (Figure 10 A, r = 0.1), the first derivative of the thermal denaturation curve is broad signal (Figure 10B, Inset, full line) – in such case, fitting of monophasic curve to sigmoidal equation model (which actually agrees with theoretical shape of curve) and consequent first derivative

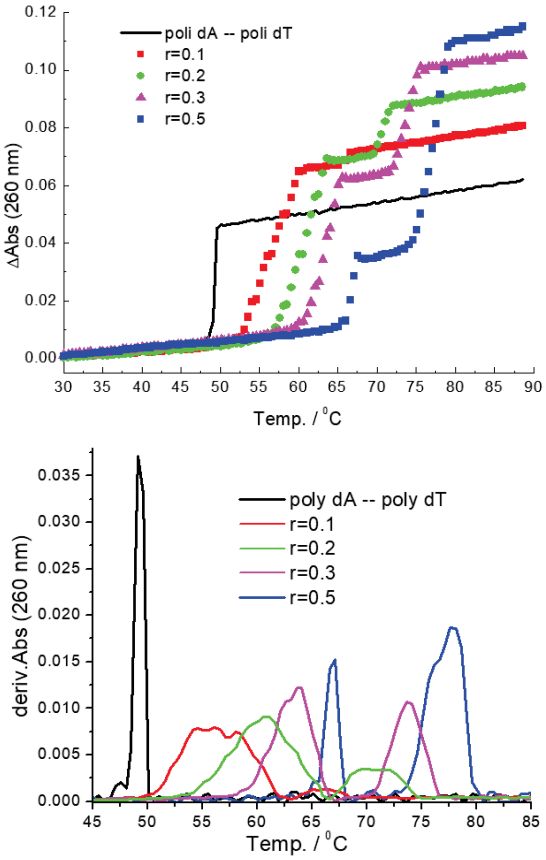

Figure 10. a) Representative thermal denaturation profiles of ligand/DNA complexes at varying ratio r = [ligand] / [DNA]: free AT-DNA (black line); predominantly single mode stabilisation (r = 0.1; red square), other curves are biphasic (indicative for two binding modes) characterised by increasing contribution of 2nd transition step at r > 0.2. b) First derivative plots of the denaturation curves shown in a); **Inset:** solid line represents the raw data derivative, dotted line corresponds to the derivative of data fitted using a sigmoidal equation.[85]

calculation (Figure 10B, Inset, dotted line) will produce better defined maximum and more accurate T_m value. If any further ligand addition above saturation ratio r does not result in any change of ΔT_m value, this strongly supports only one dominant binding mode of a ligand.

At higher ligand-to-DNA ratios, the curves frequently become biphasic, with one transition decreasing and the other increasing as r exceeds 0.2 (Figure 10), indicating the presence of two binding modes—often correlating with ligand aggregation in excess of DNA (see sections Spectrophotometric (UV-Vis or fluorimetric) Titrations and Circular Dichroism (CD) Spectroscopy). Accordingly, these data, when supported by complementary methods, can be assigned to distinct binding modes.[35]

Interpretation of Results, Limitations, and Considerations

Polystranded-DNA thermal denaturation is a complex, sequence-dependent multi-phase process influenced by DNA structural form, ion concentration, pH and other experimental conditions. During the experiment, aside denaturation, DNA can change between different conformations (e.g., A–DNA, B–DNA, Z–DNA), and the transition between these forms can complicate the interpretation of thermal denaturation curves. For that reason any DNA denaturation curves not strictly agreeing with sigmoidal shape (can be checked by fitting data to sigmoidal eq. with expected R^2 > 0.99) should be considered with caution (repeated, checked with increased DNA concentration or enhanced instrument sensitivity)

However, accurately obtained results can be related to typical binding modes, in corroboration with other methods:

Classical ligand intercalation, due to the strong aromatic stacking of a ligand with adjacent DNA-basepairs, should result in moderate to strong stabilization (ΔT_m value > 5 °C), and usually reaches saturation at *r*[ligand] / [DNA] = 0.2. Such binding mode is only partially affected by ionic strength increase (e.g. addition of NaCl).[85] It is commonly non-selective between different types of ds-DNA / RNA or different basepair content.

Ligand's electrostatic interaction with the polyanionic DNA backbone can yield a stabilization or even destabilization effect. If structurally suspected, the obtained ΔT_m value would be strongly dependent on ionic strength (e.g., addition of NaCl), to the point that increase of salt concentration by order of magnitude would completely abolish DNA stabilization by ligand.

Ligand binding into DNA minor groove commonly results in moderate to strong DNA stabilization, and it is generally strongly selective for AT–DNA in B–helical form.

Ligand aggregation within DNA binding sites (usually grooves): commonly manifested by strong effects beyond single ligand molecule saturation point (*r*[ligand] / [DNA] > 0.2). The formation of aggregate within DNA is usually dependent on electrostatic interactions, and this effect can be strongly diminished by ionic strength increase (e.g., addition of NaCl).[85]

Non-specific ligand agglomeration along DNA (commonly outer surface interactions with DNA backbone): negligible stabilization effects.

Binding Affinity

Even for ligand / DNA complex with only one binding mode and fully saturated binding sites, the ΔT_m value doesn't directly and unambiguously translate to binding affinity, especially with values determined at isothermal conditions (section Spectrophotometric (UV-Vis or fluorimetric) Titrations, room temperature). Some high–affinity binding modes (e.g. groove binding or electrostatic interaction with polyanionic DNA backbone) are dominantly based on a ligand interaction with one DNA strand and do not stabilize ds–DNA significantly, whereas classical ligand intercalation is essentially based on ligand strong aromatic stacking with basepairs, leading to strong thermal stabilization. Further, thermal denaturation is performed at increasing temperature, and for accurate thermodynamic binding constant calculation it is necessary to determine the heat capacity change (ΔC_p). Some advanced methods, like Differential Scanning Calorimetry (DSC, Supporting Information, S3.2.) can provide enthalpy changes at T_m, but even those cannot predict impact of structural DNA changes, which can affect the heat capacity change (ΔC_p). Because ignoring the eventual inaccuracy of the value of ΔC_p can introduce systematic errors when extrapolating binding constants to lower temperatures, thermal thermal denaturation methods are best suited only for estimating affinity under biologically relevant conditions and should be supported by complementary methods performed under isothermal conditions.

PITFALLS IN THERMAL DENATURATION STUDIES

Inaccurate or Too Low DNA Concentration (One of the Most Common Errors)

Problem: DNA and ligand concentrations are critical for reliable thermal denaturation curves. Errors in quantification (e.g., from impure or not completely folded oligonucleotides or inaccurate DNA absorption coefficients) directly affect shape of DNA thermal denaturation curve, intensity of hyperchromic change, as well as the reliability of applied ligand / DNA stoichiometries.

Solution: Use high-quality, HPLC-purified oligonucleotides; check DNA concentration by absorbance at exact conditions (buffer, ionic strength, pH) using sequence-specific wavelength and molar absorption coefficients (section DNA/RNA (Hosts)). Double check by DNA CD spectrum collected in the same cuvette in which thermal denaturation is to be performed (section Circular Dichroism (CD) Spectroscopy).

Buffer Mismatch and pH Drift (one of the most common errors)

Problem: Different buffers for DNA and ligand stock solution can cause artefacts. Particularly common is neglecting the impact of DMSO (from ligand stock solution) on DNA denaturation: any amount of DMSO > 0.1 % in studied solution can decrease DNA T_m considerably.

Solution: Use the same buffer for all solutions. Add adequate amount of solvent used in ligand stock solution to the free DNA sample in cuvette, to compensate impact.

Poor Mixing and Sample Inhomogeneity

Problem: Incomplete mixing of components within the cuvette can lead to sample heterogeneity and

inconsistent measurements. Additionally, during thermal denaturation, precipitation or colloidal formation may occur, resulting in unexplained shifts or abrupt changes in the thermal denaturation curve, including strong drop of absorbance.

Solution: The Ligand/DNA sample stability and homogeneity, and incubation period, should be checked in advance as described in section Spectrophotometric (UV-Vis or fluorimetric) Titrations for UV–vis titrations. After the thermal denaturation experiment, visually inspect suspecting cuvette by directing a laser pointer beam through the sample perpendicularly oriented to the eye – the presence of opalescence or visible precipitation indicates sample instability, rendering the results invalid. In such cases, the experiment should be repeated, potentially using a lower *c*(DNA).

High Baseline Drift During Heating

Problem: In ligand / DNA samples (but not in free DNA sample) the instrument readout is significantly but almost linearly changing even prior (and after) of the expected DNA thermal denaturation curve.

Solution: Likely ligand absorbs at used readout wavelength and absorbance changes with temperature. See ligand characterisation of a ligand at section Ligands (Small Molecules), and eventually correct thermal denaturation experiments for effect measured simultaneously in sample of ligand alone.

Indicator Displacement Assay (IDA)

This is an indirect method for assessing non-covalent interactions between a ligand and DNA. It is based on the principle of thermodynamic equilibrium between DNA saturated by reference small molecule (a known DNA binder, e.g., ethidium bromide), latter being progressively displaced from the DNA upon addition of the studied ligand. This displacement indicates effective binding of a ligand to DNA and can be used for the estimation of the ligand relative binding affinity. While IDA works well for the host molecule with only one binding site, common ds-DNA typically offers at least four different binding sites (Scheme 1: intercalation, minor and major groove, electrostatic binding on an outer surface of DNA). Therefore, there is no guarantee that the reference ligand and the studied ligand will bind exclusively to the same binding site. Thus, this approach is generally less accurate than the direct study of ligand / DNA interactions by spectrophotometric methods, described in sections Spectrophotometric (UV-Vis or fluorimetric) Titrations and Circular and Linear Dichroism (CD) Spectroscopy. However, it is commonly employed when those methods are not applicable or are hindered by technical limitations.[86–88] The most common reason is the study of a non-fluorescent ligand absorbing light only in the UV range with low molar absorption coefficient.

Essential Characteristics of IDA Applied on DNA Binders

Even in the case DNA binding site of reference and studied ligand are different, often displacement does effectively take place. The reason for that contra-intuitive event is that reference is non–covalently bound to DNA, meaning it permanently oscillates between binding site and bulk solution. If studied ligand by any means (for instance steric hindrance or electrostatic interaction with DNA backbone) blocks approach to reference-DNA-binding site, the reference will be displaced. Consequently, no conclusion on binding site of a ligand can be derived from IDA experiment.

The IDA may not work for sterically demanding ligands (for instance threading intercalators[9,10]), which rely on natural ds–DNA oscillations (double strand-structure folding and unfolding in μs – ms range),[12,13] since the most common reference DNA binders strongly bind to DNA and stabilise it against common DNA-structure oscillations.

Studied ligand can bind to DNA not displacing the reference ligand: typical example is reference intercalating into DNA and studied ligand electrostatically binding along DNA backbone, or ligand and reference binding in minor or major groove, respectively.[11]

PROCEDURES (IDA)

For the better comparison of Indicator displacement assay (IDA) with other methods, as well as with common practice in the literature, experiments are usually performed at very similar conditions to fluorimetric or UV-Vis / CD titrations (sections Spectrophotometric (UV-Vis or fluorimetric) Titrations or Circular and Linear Dichroism (CD) Spectroscopy), including buffer, ionic strength, concentration of DNA, standard type of quartz cuvette and eventual traces of other solvents.

Step-by-Step Protocol

Choice of a detection method: the most common is fluorescence (section Spectrophotometric (UV-Vis or fluorimetric) Titrations.), relying on a large variety of emissive DNA-binding dyes, preferably with strong emission change upon DNA binding (both, on- and off-switches are acceptable).[88] However, CD spectroscopy (section Circular and Linear Dichroism (CD) Spectroscopy) can also be used. In both cases it is essential that the signal of a reference dye does not overlap with the studied ligand (both should be adequately characterised as outlined in Ligands (Small Molecules)).

Choice of a reference dye: based on a preliminary estimation of ligand affinity toward DNA (based on a ligand structure, which could suggest binding interactions, as well as results of section Thermal Denaturation of DNA (Thermal denaturation Curves) and eventually estimations from sections Spectrophotometric (UV-Vis or fluorimetric) Titrations

or Circular and Linear Dichroism (CD) Spectroscopy), an adequate reference ligand should be used.

For instance, ethidium bromide or thiazole orange (fluorescent sensors, strong emission increase upon DNA binding[87]) would be good references for ligands with estimated K_s = 10^5–10^6 M^{-1}, suspected to intercalate in DNA. Further, DAPI, characterised by 20–30-fold fluorescence increase upon DNA binding, but also highly selective ICD sensor (strong positive band at 380 nm[DAPI[89]) for only AT–DNA minor groove, would be adequate for suspected groove binders. The DAPI binding constant for AT-DNA is within the K_s= 10^7–10^8 M^{-1} range.[90] For high-affinity ligands, with estimated K_s = 10^7–10^{10} M^{-1}, TOTO or analogues (YOYO) would be appropriate, as their fluorescence increases >1000-fold when bound to any kind of DNA.[21]

Instrument setup: taking into account all fluorescence (sections Purity and Characterization of Ligands and DNA (Host) and Spectrophotometric (UV-Vis or fluorimetric) Titrations, particularly inner filter effect – keep total A < 0.1 at excitation wavelength) or CD (section Circular and Linear Dichroism (CD) Spectroscopy, particularly total absorbance at detection wavelength) issues, instrument setup is adjusted to the highest sensitivity related to reference / DNA complex. Measuring complete spectra is recommended, it can give additional information (see Pitfalls in IDA studies - C).

Measuring reference / DNA complex: applying the known binding constant from the literature (estimated K_s for several common dyes given in section Choice of a reference dye) the ratio r = [reference] / [DNA] is adjusted to > 90 % of reference / DNA complex formed, which ensures that only negligible amount of unoccupied binding sites is available, in the same time meaning that the most of reference molecules are bound (thus giving strong signal). Measure after optimized incubation period (sections Spectrophotometric (UV-Vis or fluorimetric) Titrations or Circular and Linear Dichroism (CD) Spectroscopy).

To simplify by example, for ethidium bromide with average K_s(dsDNA) ~ 10^6 M^{-1} and the c(DNA) = 5 × 10^6 M^{-1}, c(EB) = 2 × 10^6 M^{-1} (r = 0.4).

At the same conditions used for reference / DNA complex measure the controls: DNA–only, reference–only, ligand–only, DNA–ligand (sometimes could become fluorescent or change baseline by means of scattering effects, see Ligands (Small Molecules)), reference-ligand at r = 0.1; 1 and 3 (checking if there is interaction between them); and buffer.

Titration: aliquots of the studied ligand are added starting from the ratio r [reference] / [ligand] = 0.05, progressively displacing the reference dye from DNA, and for each addition, spectra are collected. If at r = 1 the changes in spectrum are about 50 % with respect to the reference-only spectrum (collected as control in Measuring reference / DNA complex), the experiment is well-equilibrated. Any significant deviation from that (completed titration at r << 0.5 or negligible changes at r = 1) renders the experiment inapplicable.

When in doubt (for any reason outlined in section IDA or others), combine fluorescence-based assays with CD–based assays to validate displacement vs. structural change.

RESULTS (IDA)

There are several ways to present IDA data. Mathematically, it often fits a four-parameter logistic equation, and the midpoint corresponds to the IC_{50} (the concentration of the displacing ligand at which 50 % of the original ligand is displaced). The displacement curve is typically sigmoidal when you plot a percentage (%) of the displaced reference ligand versus the log concentration of the displacing ligand, and the midpoint corresponds to the IDA_{50}. An alternative, and often more intuitive, approach is to plot a percentage (%) of a reference dye–DNA complex versus the molar ratio r = [reference dye] / [ligand] (Figure 11). In this format, the IDA_{50} can be read directly at the 50 % displacement point, also providing a clear visual link between the reference dye and ligand. In such representation, $IDA_{50} \ll 1$ indicates that a large excess of ligand is required—signalling lower affinity compared to the reference dye—while $IDA_{50} \gg 1$ suggests higher affinity.

Collected IDA data (Figure 11) are therefore processed by means:

$$\% \frac{\text{reference dye}}{\text{DNA complex}} = \frac{\left(\text{Int}_{\text{dye}} / \text{ DNA} - \text{Int}_{\text{measured}}\right)}{\left(\text{Int}_{\text{dye}} / \text{ DNA} - \text{Int}_{\text{dye-only}}\right)} \cdot 100$$

$$\% \frac{\text{ligand}}{\text{DNA complex}} = 100 - \% \frac{\text{reference dye}}{\text{DNA complex}} \qquad (2)$$

where Int_{dye} / DNA is intensity of reference / DNA complex; $\text{Int}_{\text{dye-only}}$ is intensity of control reference-only spectrum and Intmeasured is a spectrum after each ligand addition. The intersection of two curves corresponds to the 50 % displaced reference: IDA_{50}.

Chosen example (Figure 11) demonstrates a common set of results and the expected non-linear shape of signal changes, whereby the ratio r = [reference] / [ligand] at 50 % displacement gives IDA_{50} value. However, these experimental results nicely demonstrate several issues that can complicate analysis of IDA assays:

- IDA_{50} values determined by using two reference dyes significantly differ (IDA_{50} = 0.3 and 1.1, respectively).
- DAPI displacement assay can be extrapolated to 0% of DAPI / DNA vs 100 % ligand / DNA (Figure 11d, dotted lines), whereas EB displacement assay cannot (Figure 11b).

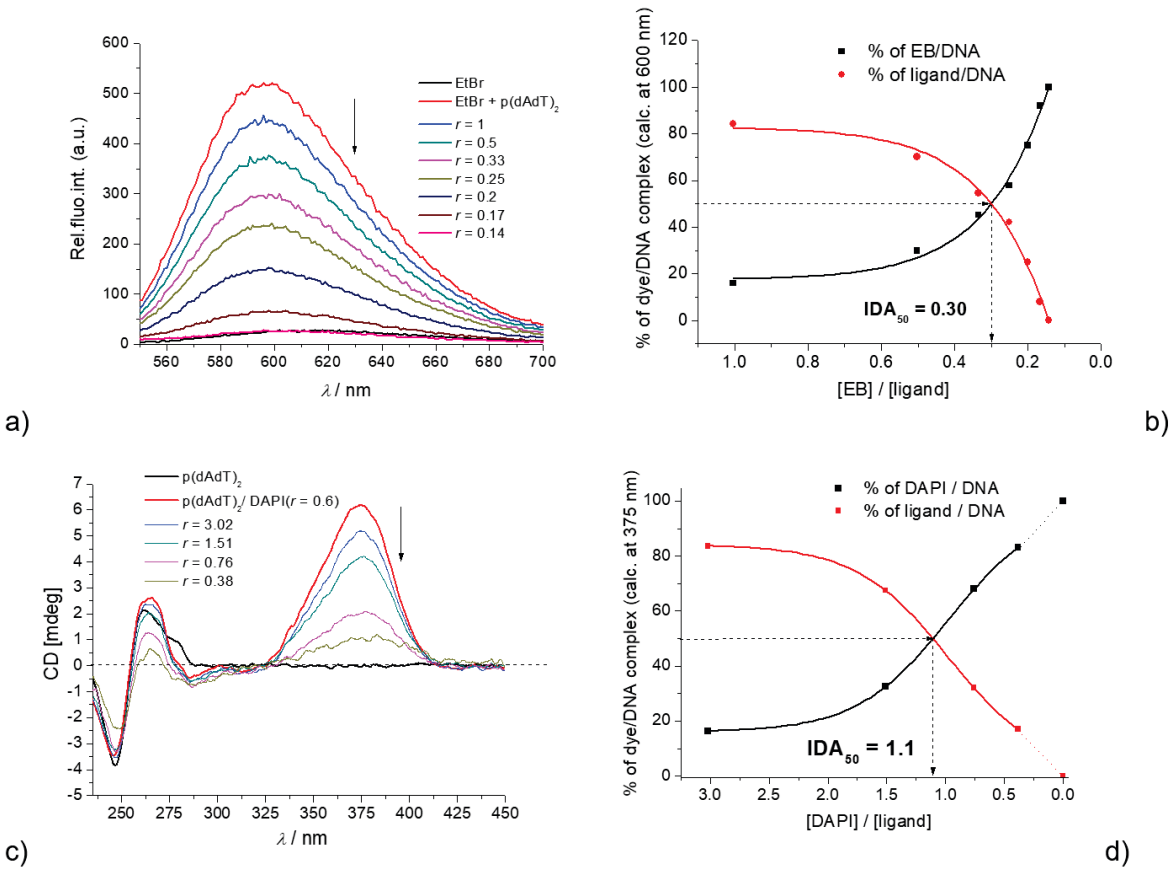

Figure 11. a) Changes in the fluorescence of ethidium bromide (c = 2 × 10^{-6} M, λ_{exc} = 520 nm, λ_{em} = 600 nm) bound to p(dAdT)$_2$ (c = 5 × 10^{-5} M) as a function of ratio r = [reference] / [ligand]; b) calculated IDA values from fluorimetric data; c) DAPI (c = 1.2 × 10^{-5} M) displacement with ligand after binding to p(dAdT)$_2$ (c = 2 × 10^{-5} M) at various ratio r = [reference] / [ligand] ; d) calculated IDA values from ICD data. Measured in sodium cacodylate buffer, pH 7, I = 0.05 M.[91]

Since chosen ligand by steric reasons cannot intercalate between DNA basepairs, and other results support its binding into DNA minor groove, presented results can be assigned as follows: displacement of DAPI from the same DNA binding site is more adequate, can be annotated by a sigmoidal curve in the complete range from 0–100 %. The intercalator EB displacement IDA$_{50}$ suggests much larger excess of ligand necessary for displacement and cannot be extrapolated to 0 % of EB bound to DNA, suggesting that even at a very high excess of a ligand, a considerable amount of EB would remain DNA-bound.

Estimation of binding affinity: if all other experimental data suggest that reference dye and ligand are bound in the same DNA binding site, under presumption that they both occupy similar length of DNA (usually expressed as Scatchard ratio n = [bound ligand] / [DNA] from section Processing of titration data to determine binding constants (K_s) and stoichiometries (Scatchard ratio n = [bound ligand]/[DNA])), rough estimation of binding affinity can be calculated :

- K_s(ligand) = K_s(reference dye) / IDA$_{50}$

PITFALLS IN IDA STUDIES

In general, previously mentioned common pitfalls (sections Pitfalls in Titration-Based DNA Binding Studies and Pitfalls in CD Titrations) should be taken into consideration. Some specifics for IDA are listed below:

Negligible signal response

Problem: No detectable displacement of reference ligand, although other methods suggest efficient ligand / DNA binding.

Solution: Choice of reference dye regarding DNA binding site: likely ligand does not bind to the same site as the reference (e.g., minor groove binder vs major groove binder[11] or intercalator). Try reference dye with a different DNA binding site, structurally accessible for the studied lig and (for instance, if a ligand is not likely to intercalate into DNA, the ethidium bromide as a reference is not recommended).

Response far away from r = [reference] /[ligand] = 1 or stalling and lack of complete displacement at high ligand excess (r < 0.1)

Problem: The change of a signal is either noticeable

at very high (r > 5) or very low (r << 0.01) ratio r = [reference] / [ligand].

Solution: i) Unmatched binding site of reference dye and ligand: likely ligand does not bind to the same site as the reference dye (e.g., minor groove binder vs major groove binder[11] or intercalator). ii) Unmatched binding affinity of reference dye and ligand: try reference dye with corresponding (lower or higher) DNA binding affinity.

Signal changes are erratic or unexpected (increase instead of decrease)

Problem: The change of a reference dye spectrum is not as expected, continuous from dye / DNAcomplex to free reference dye, but shows an unexpected shift of maximum or intensity change

Solution: likely reference dye and ligand form a complex within DNA binding site (although control experiment in subsection Measuring reference/DNA complex) did not show interaction). Try reference of a significantly different structure, less prone to aromatic stacking interactions.

CONCLUSION AND INTERPRETATION OF RESULTS

Here elaborated four methods provide a well-rounded toolkit for a general ligand / DNA interaction study, possible to perform by commonly accessible instruments in the reasonable time-frame. Spectrophotometric titrations, including UV—Vis and fluorimetric methods, are fundamental for quantifying ligand-DNA binding affinities and stoichiometries, whereas ircular dichroism (CD) spectroscopy supplements this by revealing DNA conformational changes and ligand orientation relative to the chiral DNA axis, providing clues about binding modes while also supporting binding affinity and stoichiometry assessments. Thermal denaturation assay, essentially independent method to spectrophotometric titrations, evaluates how ligand binding stabilizes DNA's structure, which correlates with binding stoichiometry and at certain conditions may relate to binding affinity. Finally, if additional support is needed due to suboptimal

Table 2. Summary of parameters and here elaborated methods results related to the DNA binding mode of studied ligand.[(a)]

	Intercalation[(b)]	Groove binding	Aggregation[(c)]	Electrostatic binding[(f)]
Structural parameters (not exclusive, just general rule)	At least two (preferably more) flat, condensed aromatics, not sterically hindered for insertion between DNA basepairs.	Flexible molecule, favourably crescent-shaped, often end-positioned positive charge(s) and DNA H-bonding ability	Two or more aromatics (not necessarily condensed), hydrophobic, prone to aggregate in water >10 μM	Highly positively charged, weakly hydrophobic, often small or no aromatic units
Spectrophotometric titrations	UV-Vis titration at er < 0.5, moderate to strong hypo- and bathochromic effect, K_s > 10^5 M^{-1}, n < 0.25,[(d)] not sensitive to ionic strength increase	UV-Vis titration at er < 0.5, weak or moderate hypo- and bathochromic effect, K_s > 10^4 M^{-1}, n < 0.3,[(d)] weakly sensitive to ionic strength increase	UV-Vis titration change at er > 1, often opposite to r < 0.5,[(e)] strong change of UV spec. shape, ev. excimer emission, may be sensitive to ionic strength	Weak or no change in UV titration, K_s > 10^4 M^{-1} , n < 0.5,[(d)]
Circular/Linear dichroism	Weak ICD band rising up to r < 0.25,[(e)] eventual decrease of DNA bands (245, 260–290 nm)	Moderate or strong ICD band rising up to r < 0.3,[(e)] weak impact of DNA bands	Bisignate, coupled ICD bands starting at r < 0.2,[(e)] impact of DNA bands	Commonly non-descript or no ICD bands. Weak to very strong (condensation) impact on DNA bands
Thermal denaturation. Complementary other methods: gDSC	ΔT_m > 3 °C at r = 0.3[(e)] (saturation), often much higher.	ΔT_m > 1 °C at er = 0.3 (saturation), often somewhat higher.	ΔT_m as a second transition at r > 0.3,[(e)] (over-saturation), may be selectively removed by ionic strength increase	ΔT_m = 0 to high, often saturation r >> 0.3,[(e)] (up to 1 or 2)
Indicator displacement assay (IDA)	Displaces referent intercalator (EB, TO or similar) with IDA50 ~ 0.1–2	Displaces referent groove binder (DAPI or similar) with IDA50 ~ 0.1–2	Influenced in IDA experiment with referent groove binder (DAPI or similar)	Displaces referent polycation (fluo-tagged spermine or similar)
Other methods[(g)]	Viscometry,[92] EMSA,[93] NMR	Raman (SERS),[94] NMR (structure of ligand/DNAcomplex)[81]	NMR(i.e.aggregate characterisation prior to DNA-binding)[85]	Raman (SERS),[52,94] ITC/DSC[95]

[(a)] Positive charge is highly favourable for any DNA binder, only few known examples are neutral.

[(b)] Valid for classical intercalation, but for partial[8] or threading[9,10] intercalation cold vary.

[(c)] Mostly second binding mode accompanying dominant one at excess of DNA (r > 1)[(e)], could be sensitive to ionic strength increase if electrostatically controlled.

[(d)] Scatchard ratio n = [bound ligand] / [DNA].

[(e)] r = [ligand] / [DNA].

[(f)] Very sensitive to ionic strength increase (add. NaCl).

[(g)] Supporting Information.

performace of afore mentioned methods, indicator displacement assays (IDA) by use a competitive binding approach involving reference dyes and ligands, can help affinity estimation and reinforce identification of binding sites.

These complementary techniques collectively offer mechanistic insights into ligand-DNA interactions, enabling detailed characterization of binding strength, mode, and structural impacts essential for understanding DNA recognition and for drug design applications. However, proposed methods are based on the indirect observation of ligand or DNA spectral properties and thus rarely produce detailed information about structure of ligand / DNA complex or fine details about thermodynamics of complexation. For advanced studies of these types, some more elaborate experimental methods are shortly listed in Supporting Information. The molecular modelling methods, essential for understanding in detail ligand / DNA interactions, are out of scope of this experiential Tutorial.

It is important to note that many ligands are composed of multiple structural units, each associated with a different DNA-binding mode. For example, intercalators are often functionalized with positively charged aliphatic chains or minor-groove-binding groups, with the aim of particular target recognition or function. The binding such hybrid constructs to various DNA can be unpredictable, and in some cases, multiple binding modes may coexist. In these situations, the methods presented here can still provide valuable insights but may not yield a definitive conclusion. For such complex cases, additional, less commonly used—and often more technically demanding—methods are available, as summarized in the Supporting Information.

Acknowledgment. Collecting the experimental data for this tutorial was partially supported by the Croatian Science Foundation under the project number HrZZ IP-2022-10-9829.

Supplementary Information. Supporting information to the paper is attached to the electronic version of the article at: https://doi.org/10.5562/cca4215.

PDF files with attached documents are best viewed with Adobe Acrobat Reader which is free and can be downloaded from Adobe's web site.

REFERENCES

[1] M. Demeunynck, C. Bailly, W. D. Wilson, *Small Molecule DNA and RNA Binders: From Synthesis to Nucleic Acid Complexes*, Wiley-VCH Verlag GmbH & Co. KGaA, **2004**.

[2] J. Schneider, *Nucleic Acids as Supramolecular Targets*, Royal Society of Chemistry, London, 2013.

[3] W. D. Wilson; Ananya Paul in *Nucleic Acids in Chemistry and Biology* (Eds. G. M. Blackburn; M. Egli; M. J. Gait; J. K. Watts) Royal Society of Chemistry, London, **2022**, 477–521. https://doi.org/10.1039/9781837671328-00477

[4] M. J. Waring, *DNA-targeting Molecules as Therapeutic Agents,* Royal Society of Chemistry, London, **2018**. https://doi.org/10.1039/9781788012928

[5] S. Neidle, *J Med Chem* **2016**, *59*, 5987–6011. https://doi.org/10.1021/acs.jmedchem.5b01835

[6] D. Reha, M. Kabelac, F. Ryjacek, J. Sponer, J. E. Sponer, M. Elstner, S. Suhai, P. Hobza, *J Am Chem Soc* **2002**, *124*, 3366–3376 https://doi.org/10.1021/ja011490d

[7] S. Neidle, *Nat Chem* **2012**, *4*, 594–595. https://doi.org/10.1038/nchem.1413

[8] D. van der Westhuizen, C. A. Slabber, M. A. Fernandes, D. F. Joubert, G. Kleinhans, C. J. van der Westhuizen, A. Stander, O. Q. Munro, D. I. Bezuidenhout, *Chem-Eur J* **2021**, 27, 8295–8307. https://doi.org/10.1002/chem.202100598

[9] I. Czerwinska, S. Sato, B. Juskowiak, S. Takenaka, *Bioorg. Med. Chem.* **2014**, *22*, 2593–2601. https://doi.org/10.1016/j.bmc.2014.03.034

[10] A. R. Smith, B. L. Iverson, *J. Am. Chem. Soc.* **2013**, *135*, 12783–12789. https://doi.org/10.1021/ja4057344

[11] W. B. Hu, C. Blecking, M. Kralj, L. Suman, I. Piantanida, T. Schrader, *Chem-Eur J* **2012**, *18*, 3589–3597. https://doi.org/10.1002/chem.201100634

[12] M. Peyrard, S. Cuesta-López, G. James, *J Biol. Phys.* **2009**, *35*, 73–89. https://doi.org/10.1007/s10867-009-9127-2

[13] P. Von Hippel, N. Johnson, A. Marcus, *Biopolymers*, **2013**, *99*, 923–954. https://doi.org/10.1002/bip.22347

[14] R. Rohs, S. M. West, A. Sosinsky, P. Liu, R. S. Mann, B. Honig, *Nature,* **2009**, *461,* 1248–1253. https://doi.org/10.1038/nature08473

[15] W. Butt, B. Lai, T. Chiu, M. Bhattarai, S. Qian, A. Bishop, J. Duan, B. Alexandrov, R. Rohs, X. He, bioRxiv. **2025** https://doi.org/10.1101/2025.01.20.633840

[16] J. B. Chaires, *Biopolymers* **2015**, *103*, 473–479. https://doi.org/10.1002/bip.22660

[17] J. B. Chaires, *Biopolymers* **1997**, *44*, 201–215. https://doi.org/10.1002/(SICI)1097-0282(1997)44:3<201::AID-BIP2>3.0.CO;2-Z

[18] E. Garcia-Espana, I. Piantanida, in *Nucleic Acids as Supramolecular Targets* (Ed. H. J. Schneider), Royal Society of Chemistry, London, **2013**, pp. 213–259. https://doi.org/10.1039/9781849737821-00213

[19] H.-J. Schneider, *Chem. Soc. Rev*. **1994**, *23*, 227. https://doi.org/10.1039/cs9942300227

[20] T. Mahata, A. Kanungo, S. Ganguly, E. Modugula, S. Choudhury, S. Pal, G. Basu, S. Dutta, *Angew. Chem. Int. Ed.*, **2016**, *55*, 7733–7736. https://doi.org/10.1002/anie.201511881

[21] H. S. Rye, S. Yue, D. E. Wemmer, M. A. Quesada, R. P. Haugland, R. A. Mathies, A. N. Glazer, *Nucleic Acids Res* **1992**, *20*, 2803–2812. https://doi.org/10.1093/nar/20.11.2803

[22] I. Piantanida, B. S. Palm, P. Cudic, M. Zinic and H. J. Schneider, *Tetrahedron* **2004**, *60*, 6225–6231. https://doi.org/10.1016/j.tet.2004.05.009

[23] V. Kostjukov, N. Khomutova, A. Lantushenko, M. Evstigneev, *Biopolymers & Cell* **2009**, *25*, 133–141. https://doi.org/10.7124/bc.0007D6

[24] P. L. Privalov, C. Crane-Robinson, *Eur Biophys J Biophy* **2017**, *46*, 203–224. https://doi.org/10.1007/s00249-016-1161-y

[25] B. Jayaram, K. McConnell, S. B. Dixit, A. Das, D. L. Beveridge, *J Comp. Chem*. **2002**, *23*, 1–14. https://doi.org/10.1002/jcc.10009

[26] P. B. Dervan, B. S. Edelson, *Curr Opin Struc Biol* **2003**, *13*, 284–299. https://doi.org/10.1016/S0959-440X(03)00081-2

[27] G. Ferguson, L. Slocombe, J. Lisgarten, D. Lisgarten, C. W. Wright, R. Talbert, R. A. Palmer, B. J. Howlin, M. Sacchi, *Acs Omega* **2025**, *10*, 18283–18290. https://doi.org/10.1021/acsomega.4c08666

[28] J. Dolenc, U. Borstnik, M. Hodoscek, J. Koller, D. Janezic, *J Mol. Struct.-Theochem* **2005**, *718*, 77–85. https://doi.org/10.1016/j.theochem.2004.12.019

[29] S. Nakagawa, A. Kimura, Y. Okamoto, *J Phys. Chem. B* **2022**, *126*, 10646–10661. https://doi.org/10.1021/acs.jpcb.2c06227

[30] J. Kypr, I. Kejnovská, D. Renciuk, M. Vorlícková, *Nucleic Acids Res.* **2009**, *37*, 1713–1725. https://doi.org/10.1093/nar/gkp026

[31] N. C. Garbett, P. A. Ragazzon, J. B. Chaires, *Nat. Prot*. **2007**, *2*, 3166–3172. https://doi.org/10.1038/nprot.2007.475

[32] A. Rodger, G. Dorrington, D. L. Ang, *Analyst* **2016**, *141*, 6490–6498. https://doi.org/10.1039/C6AN01771A

[33] T. Smidlehner, I. Piantanida, G. Pescitelli, *Beil. J. Org. Chem.* **2018**, *14*, 84–105. https://doi.org/10.3762/bjoc.14.5

[34] O. Dömötör, F. Binacchi, N. Ribeiro, N. Busto, J. Gonzalez-García, E. Garcia-España, I. Correia, É. A. Enyedy, J. Hamacek, A. Terenzi, N. Basílio, G. Barone, I. Cavaco, T. Biver, *Spectrochim. Acta A* **2025**, *327*, 125354. https://doi.org/10.1016/j.saa.2024.125354

[35] J. L. Mergny, L. Lacroix, *Oligonucleotides* **2003**, *13*, 515–537. https://doi.org/10.1089/154545703322860825

[36] J. B. Chaires, M. J. Waring, *Drug-Nucleic Acid Interactions, Methods in Enzymology*, Academic Press, San Diego, **2001**, *340*, 1–705.

[37] J. G. Pelton, D. E. Wemmer, *Proc. Nat. Acad. Sci. USA* **1989**, *86*, 5723–2727. https://doi.org/10.1073/pnas.86.15.5723

[38] B. S. P. Reddy, S. K. Sharma, J. W. Lown, *Curr. Med. Chem.* **2001**, *8*, 475–508. https://doi.org/10.2174/0929867003373292

[39] P. B. Dervan, B. S. Edelson, *Curr Opin Struc Biol* **2003**, *13*, 284–299. https://doi.org/10.1016/S0959-440X(03)00081-2

[40] J. F. Escara, J. R. Hutton, *Biopolymers* **1980**, *19*, 1315–1327. https://doi.org/10.1002/bip.1980.360190708

[41] J. R. Lakowicz, *Principles of Fluorescence Spectroscopy*, 3rd ed., Springer-Verlag US, Boston, **2006**. https://doi.org/10.1007/978-0-387-46312-4

[42] H. T. Zhang, R. Li, Z. Yang, C.-X. Yin, M. R. Gray, C. Bohne, *Photochem. Photobiol. Sci.* **2014**, *13*, 917–928. https://doi.org/10.1039/c4pp00069b

[43] T. Wang, L. H. Zeng, D. L. Li, *Appl. Spec. Rev.* **2017**, *52*, 883–908. https://doi.org/10.1080/05704928.2017.1345758

[44] V. Masilamani, H. M. Ghaithan, M. J. Aljaafreh, A. Ahmed, R. al Thagafi, S. Prasad, M. S. Alsalhi, *Journal of Spectroscopy* **2017**, 4289830. https://doi.org/10.1155/2017/4289830

[45] D. I. C. Kells, J. D. J. Oneil, T. Hofmann, *Anal. Biochem.* **1984**, *139*, 316–318. https://doi.org/10.1016/0003-2697(84)90010-1

[46] L. Tan, W. Du, Y. Zhang, L.-J. Tang, J.-H. Jiang, R.-Q. Yu, *Chemometrics, Intelligent Lab. Systems*, **2020**, *203*, 104028. https://doi.org/10.1016/j.chemolab.2020.104028

[47] N. Berova, L. Di Bari, G. Pescitelli, *Chem. Soc. Rev.* **2007**, *36*, 914–931. https://doi.org/10.1039/b515476f

[48] G. Pescitelli, L. Bari, N. Berova, *Chem. Soc. Rev.* **2014**, *43*, 5211–5233. https://doi.org/10.1039/C4CS00104D

[49] B. C. Du, J. C. Yi, H. Yan, T. Wang, *Chem Eur J* **2021**, *27*, 2908–2919. https://doi.org/10.1002/chem.202002559

[50] C. R., Cantor, P. R. Schimmel, in *Biophysical Chemistry*, Vol. 3, W.H. Freeman, San Francisco, **1980**.

[51] T. Biver, *Appl Spectrosc Rev* **2012**, *47*, 272–325. https://doi.org/10.1080/05704928.2011.641044

[52] M. Ferger, Z. Ban, I. Krošl, S. Tomić, L. Dietrich, S. Lorenzen, F. Rauch, D. Sieh, A. Friedrich, S. Griesbeck, A. Kendel, S. Miljanić, I. Piantanida, T. B. Marder, *Chem Eur J.* **2021**, *27*, 5142–5159. https://doi.org/10.1002/chem.202005141

[53] M.-A. Mycek, B. W. Pogue, in *Handbook of Biomedical Fluorescence*, CRC Press, Boca Raton, United States, **2019**, ch. 3, pp. 61–105.

[54] P. Jana, F. Supljika, C. Schmuck, I. Piantanida, *Beil. J Org. Chem.* **2020**, *16*, 2201–2211. https://doi.org/10.3762/bjoc.16.185

[55] I. Piantanida, B. S. Palm, M. Zinic, H. J. Schneider, *J Chem Soc Perk T 2*, **2001**, 1808–1816. https://doi.org/10.1039/b103214n

[56] J. Lah, G. Vesnaver, *Journal of Molecular Biology* **2004**, *342*, 73–89. https://doi.org/10.1016/j.jmb.2004.07.005

[57] H. Gampp, M. Maeder, C. J. Meyer, A. D. Zuberbuhler, *Talanta* **1985**, *32*, 257–264. https://doi.org/10.1016/0039-9140(85)80077-1

[58] D. B. Hibbert, P. Thordarson, *Chem. Comm.* **2016**, *52*, 12792–12805. https://doi.org/10.1039/C6CC03888C

[59] F. Ulatowski, K. Dąbrowa,T. Bałakier, J. Jurczak, *J. Org. Chem.* **2016**, *81*, 1746–1756. https://doi.org/10.1021/acs.joc.5b02909

[60] J. Tellinghuisen, *J. Phys. Chem. B* **2007**, *111*, 11531–11537. https://doi.org/10.1021/jp074515p

[61] P. Thordarson, *Chemical Society Reviews* **2011**, *40*, 1305–1323. https://doi.org/10.1039/C0CS00062K

[62] R. B. Martin, *J Chem. Edu.* **1997**, *74*, 1238. https://doi.org/10.1021/ed074p1238

[63] P. Gans, A. Sabatini, A. Vacca, *Talanta* **1996**, *43*, 1739–1753. https://doi.org/10.1016/0039-9140(96)01958-3

[64] M. Maeder, A. D. Zuberbuhler, *Anal. Chem* **1990**, *62*, 2220–2224. https://doi.org/10.1021/ac00219a013

[65] A. N. Meshkov, G. A. Gamov, *Talanta* **2019**, *198*, 200–205. https://doi.org/10.1016/j.talanta.2019.01.107

[66] Jplus Consulting, jplusconsulting.com.

[67] J. Lah, I. Drobnak, M. Dolinar, G. Vesnaver, *Nucleic Acids Research* **2008**, *36*, 897–904. https://doi.org/10.1093/nar/gkm1110

[68] I. Crnolatac, L. Giestas, G. Horvat, A. J. Parola, I. Piantanida, *Chemosensors* **2020**, *8,* 129. https://doi.org/10.3390/chemosensors8040129

[69] S. R. Krishnan, A. Roy, M. M. Gromiha, *Briefings in Bioinformatics* **2024**, *25*, ARTN bbae002. https://doi.org/10.1093/bib/bbae002

[70] K. Harini, D. Kihara, M. M. Gromiha, *Methods* **2023**, *213*, 10–17. https://doi.org/10.1016/j.ymeth.2023.03.002

[71] L. Chen, G. A. Calin, S. X. Zhang, *J Chem. Info Model* **2012**, *52*, 2741–2753. https://doi.org/10.1021/ci300320t

[72] Y. Y. Feng, K. Q. Zhang, Q. L. Wu, S. Y. Huang, *J Chem. Info Model* **2021**, *61*, 4771–4782. https://doi.org/10.1021/acs.jcim.1c00341

[73] K. Kanahashi, M. Urushihara, K. Yamaguchi, *Scientific Reports* **2022**, *12*, Artn 11159. https://doi.org/10.1038/s41598-022-15300-9

[74] F. Zahariev, T. Ash, E. Karunaratne, E. Stender, M. S. Gordon, T. L. Windus, M. P. García, *J. Chem. Phys.* **2024**, *160*, Artn 042502 https://doi.org/10.1063/5.0176000

[75] N. Berova, L. Di Bari, G. Pescitelli, *Chem. Soc. Rev.* **2007**, *36*, 914–931. https://doi.org/10.1039/b515476f

[76] N. Berova, P. L. Polavarapu, K. Nakanishi, R. W. Woody, in *Comprehensive Chiroptical Spectroscopy: Applications in Stereochemical Analysis of Synthetic Compounds, Natural Products, Biomolecules*, Vol 2, Wiley & Sons, New York, **2012**, pp. 575–586. https://doi.org/10.1002/9781118120392

[77] M. Eriksson, B. Nordén, in *Linear, Circular Dichroism of Drug-Nucleic Acid Complexes*, *Methods in Enzymology*, (Eds. J. B. Chaires, M. J. Waring) Academic Press, San Diego, **2001**, 340, pp. 68–98. https://doi.org/10.1016/S0076-6879(01)40418-6

[78] L.-M. Tumir, I. Crnolatac, T. Deligeorgiev, A. Vasilev, S. Kaloyanova, M. G. Branilović, S. Tomić, I. Piantanida, *Chem. Eur. J.*, **2012**, *18*, 3859–3864. https://doi.org/10.1002/chem.201102968

[79] B. A. Armitage, *Top. Curr. Chem.* **2005**, *253*, 55.

[80] S. Basak, J. C. Léon, A. Ferranco, R. Sharma, M. Hebenbrock, A. Lough, J. Müller, H. B. Kraatz, *Chem. Eur. J.* **2018**, *24*, 3729–3732. https://doi.org/10.1002/chem.201800440

[81] I. Crnolatac, I. Rogan, B. Majic, S. Tomic, T. Deligeorgiev, G. Horvat, D. Makuc, J. Plavec, G. Pescitelli, I. Piantanida, *Anal. Chim. Acta* **2016**, *940*, 128–135. https://doi.org/10.1016/j.aca.2016.08.021

[82] M. Radic Stojkovic, J. Gonzalez-Garcia, F. Supljika, C. Galiana-Rosello, L. Guijarro, S. A. Gazze, L. W. Francis, I. Piantanida, E. Garcia-Espana, *Int J Biol Macromol.* **2018**, *109*, 143–151. https://doi.org/10.1016/j.ijbiomac.2017.11.156

[83] D. Jaksic, M. S. Klaric, I. Crnolatac, N. S. Vujicic, V. Smrecki, M. Gorecki, G. Pescitelli, I. Piantanida, *Marine Drugs* **2019**, *17.* 629. https://doi.org/10.3390/md17110629

[84] L. M. Aufdembrink, T. G. Hoog, M. R. Pawlak, B. F. Bachan, J. M. Heili, A. E. Engelhart, *RNA Recognition* **2019**, *623*, 23–43. https://doi.org/10.1016/bs.mie.2019.05.029

[85] I. Piantanida, B. S. Palm, M. Zinic, H. J. Schneider, *J Chem Soc Perk T 2*, **2001**, 1808–1816. https://doi.org/10.1039/b103214n

[86] D. L. Boger, B. E. Fink, S. R. Brunette, W. C. Tse, M. P. Hedrick, *J Am Chem Soc* **2001**, *123*, 5878–5891. https://doi.org/10.1021/ja010041a

[87] W. C. Tse, D. L. Boger, *Acc Chem Res* **2004**, *37*, 61–69. https://doi.org/10.1021/ar030113y

[88] A. C. Sedgwick, J. T. Brewster, T. Wu, X. Feng, S. D. Bull, X. Qian, J. L. Sessler, T. D. James, E. V. Anslyn, X. Sun, *Chem Soc Rev* **2021**, *50*, 9. https://doi.org/10.1039/C9CS00538B

[89] N. Holmgaard List, J. Knoops, J. Rubio-Magnieto, J. Ide, D. Beljonne, P. Norman, M. Surin, M. Linares, *J Am Chem Soc* **2017**, *139*, 14947–14953. https://doi.org/10.1021/jacs.7b05994

[90] a) L. A. Reis, M. S. Rocha, *Biopolymers* **2017**, *107*, e23015; https://doi.org/10.1002/bip.23015
b) S. Y. Breusegem, R. M. Clegg, F. G. Loontiens, *J Mol. Biol.* **2002**, *315*, 1049–1061. https://doi.org/10.1006/jmbi.2001.5301

[91] Unpublished data, used for demonstration of principle only.

[92] E. C. Long, J. K. Barton, *Acc. Chem. Res.* **1990**, *23* 271–273. https://doi.org/10.1021/ar00177a001

[93] S. M. Zeman, D. M. Crothers in *Methods in Enzymology*, Vol. 340 (Eds.: J. B. Chaires, M. J. Waring), Academic Press, San Diego, **2001**, pp. 51–68. https://doi.org/10.1016/S0076-6879(01)40417-4

[94] E. Garcia-Rico, R. A. Alvarez-Puebla, L. Guerrini, *Chem Soc Rev* **2018**, *47*, 4909–4923. https://doi.org/10.1039/C7CS00809K

[95] T. C. Choma in *Characterizing non-covalent nucleic acid interactions with small molecules, proteins by calorimetry,* TA Instruments, New Castle, DE, USA. https://www.tainstruments.com/pdf/literature/M577_Nucleic%20acid%20interactions.pdf